



Nitrogen and phosphorus cycling in an ombrotrophic peatland: a benchmark for assessing change

Verity G. Salmon · Deanne J. Brice · Scott Bridgman · Joanne Childs · Jake Graham · Natalie A. Griffiths · Kirsten Hofmockel · Colleen M. Iversen · Terri M. Jicha · Randy K. Kolka · Joel E. Kostka · Avni Malhotra · Richard J. Norby · Jana R. Phillips · Daniel Ricciuto · Christopher W. Schadt · Stephen D. Sebestyen · Xiaoying Shi · Anthony P. Walker · Jeffrey M. Warren · David J. Weston · Xiaojuan Yang · Paul J. Hanson

Received: 3 December 2020 / Accepted: 23 June 2021
© The Author(s), under exclusive licence to Springer Nature Switzerland AG 2021

Abstract

Aims Slow decomposition and isolation from groundwater mean that ombrotrophic peatlands store a large amount of soil carbon (C) but have low availability of nitrogen (N) and phosphorus (P). To better understand the role these limiting nutrients play in determining the C balance of peatland ecosystems,

we compile comprehensive N and P budgets for a forested bog in northern Minnesota, USA.

Methods N and P within plants, soils, and water are quantified based on field measurements. The resulting empirical dataset are then compared to modern-day, site-level simulations from the peatland land surface version of the Energy Exascale Earth System Model (ELM-SPRUCE).

Communicated by Manuel Delgado-Baquerizo.

V. G. Salmon (✉) · D. J. Brice · J. Childs · N. A. Griffiths · C. M. Iversen · R. J. Norby · J. R. Phillips · D. Ricciuto · X. Shi · A. P. Walker · J. M. Warren · X. Yang · P. J. Hanson
Climate Change Science Institute and Environmental Sciences Division, Oak Ridge National Laboratory, Oak Ridge, TN, USA
e-mail: salmonvg@ornl.gov

S. Bridgman
Institute of Ecology and Evolution, University of Oregon, Eugene, OR, USA

J. Graham
Department of Geosciences, Boise State University, Boise, ID, USA

K. Hofmockel
Earth and Biological Sciences Directorate Molecular Science Laboratory, Pacific Northwest National Laboratory, Richland, WA, USA

K. Hofmockel
Department of Ecology, Evolution, and Organismal Biology, Iowa State University, Ames, IA, USA

T. M. Jicha
US Environmental Protection Agency, Office of Research and Development, National Health and Environmental Effects Laboratory, Mid-Continent Ecology Division, Center for Computational Toxicology and Exposure, Great Lakes Toxicology and Ecology Division, Duluth, MN, USA

R. K. Kolka · S. D. Sebestyen
USDA Forest Service Northern Research Station, Grand Rapids, MN, USA

J. E. Kostka
School of Biological Sciences, Georgia Institute of Technology, Atlanta, GA, USA

A. Malhotra
Department of Earth System Science, Stanford University, Stanford, CA, USA

R. J. Norby
Department of Ecology and Evolutionary Biology, University of Tennessee, Knoxville, TN, USA

Results Our results reveal N is accumulating in the ecosystem at $0.2 \pm 0.1 \text{ g N m}^{-2} \text{ year}^{-1}$ but annual P inputs to this ecosystem are balanced by losses. Biomass stoichiometry indicates that plant functional types differ in N versus P limitation, with trees exhibiting a stronger N limitation than ericaceous shrubs or *Sphagnum* moss. High biomass and productivity of *Sphagnum* results in the moss layer storing and cycling a large proportion of plant N and P. Comparing our empirically-derived nutrient budgets to ELM-SPRUCE shows the model captures N cycling within dominant plant functional types well.

Conclusions The nutrient budgets and stoichiometry presented serve as a baseline for quantifying the nutrient cycling response of peatland ecosystems to both observed and simulated climate change. Our analysis improves our understanding of N and P dynamics within nutrient-limited peatlands and represents a crucial step toward improving C-cycle projections into the twenty-first century.

Keywords Peatland · *Sphagnum* · *Picea mariana* · Peat · Belowground · Stoichiometry

Introduction

Peatlands are often nutrient-limited, carbon (C) rich ecosystems with variable microtopography, biogeochemistry, and hydrology. They store an estimated 33–50% of global soil C due to productivity historically outpacing decomposition in these cold, acidic, and frequently waterlogged soils (Yu 2012; Scharlemann et al. 2014; Nichols and Peteet 2019). Slow decomposition also contributes to low availability of critical nutrients like nitrogen (N) and phosphorus (P). Ombrotrophic peatlands receive inputs of nutrients only through atmospheric deposition and N fixation, making them more nutrient-limited than minerotrophic peatlands, which can also be supplied with nutrients in runoff and groundwater (Bridgman et al. 1998). Our understanding of nutrient limitation within peatland ecosystems has been heavily informed by fertilization experiments. However,

the response of peatland vegetation to fertilization is often strongly dependent on site-level hydrology, alkalinity, and nutrient availability (Bridgman et al. 1996). Fertilization experiments conducted across a gradient of ombrotrophic to minerotrophic peatlands revealed tradeoffs between nutrient residence times in plants and nutrient allocation to productivity (Iversen et al. 2010). At two ombrotrophic peatlands (bogs) in Sweden, fertilization treatments revealed that N and P can be co-limiting, with N limiting productivity in places where N deposition rates are low and P limiting productivity where N deposition rates are high (Aerts et al. 1992). To understand the future C dynamics of bogs, it is therefore critically important to consider not only the availability of soil-derived N and P but also storage, turnover, deposition, and loss of these potentially co-limiting nutrients.

Stoichiometry, the relative balance of elements like N and P in ecosystem pools and fluxes, can provide valuable insight into the equilibrium between nutrient demand and nutrient availability (Vitousek 1982; Sterner and Elser 2002). Plant stoichiometry has long been used to infer potential limitations of nutrient availability on rates of primary production (Güsewell 2004). However, these stoichiometric models involve only the relative elemental ratios of ecosystem components and can therefore be limited in their scope and interpretation (Reiners 1986). Though this simplification can hide many important ecological processes, stoichiometric models can be used to capture ecosystem outcomes across space and through time, as well as within the abiotic and biotic components of the ecosystem. Stoichiometric data are also relatively simple to obtain and are therefore widely available for parameterization. This flexibility is one reason why stoichiometric relationships are a crucial part of many Earth System Models (ESMs) as a way to represent nutrient mineralization, immobilization, and limitation to growth (Thomas et al. 2015; Achat et al. 2016). Changes in nutrient availability and demand that are caused by shifts in plant community composition or altered climate can, however, alter ecosystem stoichiometry as plant functional types (PFTs) may respond differently to changing environmental conditions (Elser et al. 2010).

Here we present detailed N and P nutrient budgets and a stoichiometric analysis of a boreal ombrotrophic bog located at the USDA Forest Service's Marcell Experimental Forest in north central

C. W. Schadt · D. J. Weston
Climate Change Science Institute and Biosciences
Division, Oak Ridge National Laboratory, Oak Ridge, TN,
USA

Minnesota, USA. This northern peatland represents a globally relevant pool of soil C that may be vulnerable to accelerated decomposition under climate change (Wu et al. 2013; Hanson et al. 2020; Hopple et al. 2020). Carbon stored in peat has the potential to fuel a positive feedback to climate if released to the atmosphere in the form of carbon dioxide or methane (Frolking and Roulet 2007). Accurate representation of N and P cycling through the peat, vegetation, and water of ombrotrophic bogs is crucial part of developing mechanistic ESMs that produce sound long term climate projections. The goals of our analysis are therefore as follows:

1. Evaluate the distribution of N and P in an ombrotrophic peatland ecosystem under ambient conditions.
2. Quantify N and P fluxes into and out of the peatland ecosystem.
3. Contrast field observations of N and P cycling to pools and fluxes from land surface components of an ESM.

The resulting analysis will serve both as an important baseline for ESMs and an important reference point for quantifying changes in the N:P stoichiometry of this ombrotrophic bog in response to both gradual climate change in the region as well as experimental temperature and atmospheric CO₂ treatments currently being implemented at the site. Throughout this analysis, plant species are grouped into PFTs according to their functional similarity to facilitate comparison with ESM output. PFTs in the understory consist of forbs, sedges, and shrubs while trees make up the overstory. *Sphagnum* moss, a non-vascular PFT, has been developed as a new PFT in ELM-SPRUCE because of its crucial role in peatland ecology.

Methods

Site description

The USDA Forest Service Marcell Experimental Forest (MEF) is located in Minnesota, USA (47° 30.476' N; 93° 27.162' W). The MEF has a mean annual temperature of 3.5 °C, and precipitation averages 787 mm

per year (Sebestyén et al. 2021a, b). MEF is comprised of upland forests, fens, bogs, and lakes (Kolka et al. 2011). This study took place in the S1 Bog, which is an 8.1-ha raised-dome, ombrotrophic peatland surrounded by a lagg zone. Upland waters contribute water and nutrients to the lagg, but in the central peatland, atmospheric deposition and N fixation provide the only nutrient inputs. The pH of the bog near-surface porewater ranges from 3.4–4.0 (Griffiths and Sebestyén 2016). The organic soils at the S1 Bog are typically 1–5 m in depth and are characterized as Dysic, frigid Typic Haplohemist (Greenwood series; <http://websoilsurvey.nrcs.usda.gov>), indicating that the peat column is predominantly hemic in nature. The tree canopy at S1 Bog is approximately 8-m high and dominated by *Picea mariana* (Mill., black spruce, herein *Picea*) and *Larix laricina* (Du Roi, eastern larch, herein *Larix*). The understory consists of ericaceous shrubs (primarily *Chamaedaphne calyculata* (L.), *Rhododendron groenlandicum* (Oeder), *Vaccinium angustifolium* (Aiton)) and a dense covering of moss [*Sphagnum magellanicum* (Brid.), *S. fallax* (H. Klinggr), *S. angustifolium* (Warnst), *Polytrichum* spp.] as well as various sedges and forbs.

The S1 Bog represents natural regrowth following experimental clear-cuts in 1969 and 1974 (Sebestyén et al. 2011). The plant community at S1 Bog is likely continuing to stabilize following these clear-cuts since black spruce bogs in Alberta have taken 90 years to stabilize following fire (Wieder et al. 2009). Tree basal area at the S1 Bog, however, is similar to observations made prior to the clear-cuts (7 cm² m⁻²; Verry 2018 data citation; Jensen et al. 2019). Carrying on MEF's legacy of manipulative experiments, the S1 Bog is currently home to the U. S. Department of Energy's Spruce and Peatland Responses Under Changing Environments (SPRUCE) Experiment. At SPRUCE, temperature and atmospheric CO₂ are manipulated in a regression design to inform our understanding of how this C-rich ecosystem will respond to future climate (Griffiths et al. 2017; Hanson et al. 2017, 2020).

The present analysis encompasses conditions at the S1 Bog prior to the implementation of the SPRUCE manipulative treatments. Measurements were either made within the footprint of SPRUCE plots prior to treatment implementation or, in the case of ambient plots, represent an ongoing record of unmanipulated

conditions within plots that are not encircled by an enclosure (henceforth ‘ambient plots’). In a few instances, data from enclosed but unwarmed plots were used, as noted below. The spatial and temporal window over which N and P data are available varies widely across datasets. Most measurements were compiled at the scale of SPRUCE plots: octagonal areas encompassing 66.4 m² (Hanson et al. 2017). The citations, plots, years, and units of replication for each measurement are listed in Table 1 and DOI links for publicly available data are listed under ‘References to data products and documentation.’

Peat stocks

In 2012, soil cores were collected in the SPRUCE plots to capture pre-treatment peat C and nutrient stocks (Table 1; Iversen et al. 2014 data citation). Raised hummock and depressed hollow microtopographic features within each plot were cored (one core per feature), and cores were separated into roughly 10-cm depth increments from 0–100 cm and 25-cm depth increments from 100–200 cm. The bottom of hollows was considered to have a depth of 0 cm. For each depth interval, water content, bulk density, and %N and %P were quantified. We assumed the first depth interval encompassed the living portion of the *Sphagnum* layer. Peat from the bottom of the live *Sphagnum* layer to a depth of 30 cm was considered part of the transiently oxic acrotelm. Peat from 30–80 cm depths was considered the mesotelm transition zone, and peat from 80 to 200 cm depth was considered the anoxic catotelm [as in Verry et al. (2011); Tfaily et al. (2014)]. N and P stocks per m² of the live *Sphagnum* layer, acrotelm, mesotelm, and catotelm were calculated for both hummocks and hollows within each plot. The hummock and hollow data per plot were then combined into area-weighted averages based on the average spatial coverage of hummocks as determined by terrestrial lidar scans (67% hummock; Graham et al. 2019 data citation).

Tree biomass and production

Tree diameter at breast height (DBH) was annually surveyed in SPRUCE plots (Table 1; Hanson et al. 2018a data citation). Aboveground biomass for each year was calculated for each tree using site-specific allometric equations developed from

individual tree harvests performed in 2010, 2011, and 2016. Linear allometric relationships were fit using ordinary least squares and the intercept was forced through zero:

$$\text{Biomass} = S \times [BA \times H]$$

where S is the model slope (units g m⁻³), BA is basal area measured at 1.3 m height (m²), H is tree height (m). These allometries (Supplemental Table 1) revise those reported by (Griffiths et al. 2017) by adding 2016 harvest data and separating total aboveground biomass by species and tissue type (total aboveground biomass, branch biomass, needle biomass). Branch biomass included both needles and woody branch material. Bole biomass was therefore calculated as the total aboveground biomass minus branch biomass. Coarse-root biomass for *Picea* and *Larix* trees was calculated based on species-specific allometric equations developed for northern Manitoba, Canada by Bond-Lamberty et al. (2002).

Annual production of tree bole, woody branches, and coarse roots was considered the annual increment seen in these biomass pools. For deciduous *Larix*, annual production of needles was considered the entire needle biomass pool. For evergreen *Picea*, we assumed a 5-year needle lifespan (Lamhamedi and Bernier 1994; Jensen et al. 2015) and assume that 20% (one cohort) cycles annually. We did not take into account the production of woody litter or coarse woody debris as it is negligible in this relatively young, aggrading forest.

N and P content of tree biomass and net primary production (NPP) were calculated based on species-specific %N and %P of leaves and woody tissues. Plant tissue chemistry data were from pretreatment surveys across the S1 Bog prior to the construction of the SPRUCE experiment as well as harvests in ambient SPRUCE plots (Table 1; Philips et al. 2017 data citation, Jensen et al. 2018 data citation, Philips et al. 2021 data citation). Calculations regarding tree fine-root biomass and productivity are detailed below.

Vascular understory biomass and production

Annual harvests of 0.25 m² quadrats of understory vascular plants were performed at the S1 Bog as part of the SPRUCE experiment (Hanson et al. 2018b

Table 1 Data sources, location, and timing of measurements at the S1 Bog

Variable	References	Access	Years	Plots	Replicate unit	n =
Peat C, N and P stocks	Iversen et al. (2014 <i>data citation</i>)	https://doi.org/10.3334/CDIAC/spruce.005	2012	4,5,6,7,8,9,10,11,13,14,15,16,17,19,20,21	Plot	16
Hummock versus hollow micro-topography	Graham et al. (2019 <i>data citation</i>)	https://doi.org/10.25581/spruce.067/1515552	2016	Average across all plots used		
Tree Above-ground Biomass	Hanson et al. (2018a <i>data citation</i>)	https://doi.org/10.25581/spruce.051/1433836	2013–2020	1,2,3,5,7,9,12,14,15,18,21	Plot	11
			2013–2015	4,6,8,10,11,13,16,17,19,20	Plot	10
Understory vascular plant aboveground biomass & production	Hanson et al. (2018b <i>data citation</i>)	https://doi.org/10.25581/spruce.052/1433837	2012–2015	2,4,6,8,10,11,13,16,17,19,20	Plot	11
			2012–2018	5,7,9,14,15,21	Plot	6
Shrub coarse roots	Philips and Hanson	This paper Supplemental Table 2	2017	5,7,9,14,15,21	Plot	6
Fine root biomass	Iversen et al. (2018a)	https://doi.org/10.1007/s11104-017-3231-z	2012	4,13,16	Plot	3
Fine root production: minirhizotron measurements	Iversen et al. (2018a)	https://doi.org/10.1007/s11104-017-3231-z	2011–2012	Sampling locations A through F	Sampling location	6
Fine root production: ingrowth core measurements	Iversen et al. (2021 <i>data citation</i>)	https://doi.org/10.25581/spruce.091/1782483	2013	Sampling locations A through F	Sampling location	6
	Malhotra et al. (2020a, b)	https://doi.org/10.1073/pnas.2003361117	2015–2016	7,21	Plot	2
Sphagnum biomass	Iversen et al. (2014 <i>data citation</i>)	https://doi.org/10.3334/CDIAC/spruce.005	2012	4,5,6,7,8,9,10,11,13,14,15,16,17,19,20,21	Plot	16
Sphagnum production	Norby and Childs (2018 <i>data citation</i>)	https://doi.org/10.25581/spruce.049/1426474	2016–2017	7,21	Plot	2
Porewater total N & total P	Griffiths and Sebestyen (2016)		2011–2013	4,5,6,7,8,9,10,11,13,14,15,16,17,18,19,20	Plot	14
Bulk deposition of total N	Sebestyen et al. (2020 <i>data citation</i>)	https://doi.org/10.25581/spruce.085/1664397	2014–2018	Whole S1 bog	Year	5
Bulk deposition of total P	Ppt volume Sebestyen et al. (2020 <i>data citation</i>)	https://doi.org/10.25581/spruce.085/1664397	2014–2019	Whole S1 bog	Year	6
	TP concentration from published studies in the region	Literature Review (This paper Supplemental Table 4)				

Table 1 (continued)

Variable	References	Access	Years	Plots	Replicate unit	n =
Lateral outflow total N and Total P	Sebestyen et al. (2021a, b <i>data citation</i>)	https://doi.org/10.25581/spruce.088/1775142	2017–2018	6	Year	2
Annual nitrogen fixation	Carrell et al. (2019)	https://doi.org/10.1111/gcb.14715	2017	6	Incubation	5
	Hanson et al. (2015 <i>data citation</i>)	http://dx.doi.org/10.3334/CDIAC/spruce.001	2011–2013	6 pretreatment sampling locations	Whole S1 bog	1
	Q ₁₀ Urban and Eisenreich (1988)	https://doi.org/10.1139/b88-069	1981–1982	Whole S2 bog	Whole S2 bog	
Denitrification	Urban et al. (1988)	https://doi.org/10.4319/lo.1988.33.6part2.1611		S2 Bog		
Ammonia volatilization	Bridgham (Supplemental Fig. 2)	This paper Supplemental Fig. 2	2018, 2019	21	Plot	1
Seasonal snow cover & phenology	Heiderman et al. (2018 <i>data citation</i>)	https://doi.org/10.25581/spruce.054/1444106	2010–2017	Whole S1 bog	Whole S1 bog	1
Foliar %N, %P	Philips et al. (2017 <i>data citation</i>)	http://dx.doi.org/10.3334/CDIAC/spruce.038	2009, 2012, 2013	Survey points, 7,21		
	Philips et al. (2021 <i>data citation</i>)	https://doi.org/10.25581/spruce.090/1780604	2017–2018	5,7,9,14,15,21		
	Jensen et al. (2018 <i>data citation</i>)	https://doi.org/10.3334/CDIAC/spruce.008	2010–2015	NA		
Stem %N, %P	Philips et al. (2021 <i>data citation</i>)	http://dx.doi.org/10.3334/CDIAC/spruce.038	2009,2012,2013	Survey points, 7,21		
	Philips et al. (2021 <i>data citation</i>)	https://doi.org/10.25581/spruce.090/1780604	2017–2018	5,7,9,14,15,21		
Sphagnum %N and %P	Norby et al. (2020 <i>data citation</i>)	https://doi.org/10.25581/spruce.084/1647361	2017	7,21		
Fine root %N, %P	Iversen et al. (2021 <i>data citation</i>)	https://doi.org/10.25581/spruce.091/1782483	2013			
	Malhotra et al. (2020a)	https://doi.org/10.1073/pnas.2003361117	2015–2016	7,21		

data citation). Harvests were conducted annually in August, and vascular plant material was clipped at the green moss surface. All materials were then sorted by

species, tissue type (stem versus leaf) and tissue age (current year versus older growth). Two harvests were performed per plot at paired hummock and hollow

locations to capture microtopographic variation. After sorting, tissues were oven-dried and weighed to determine aboveground biomass (g m^{-2}) and annual aboveground production ($\text{g m}^{-2} \text{ year}^{-1}$). These values were combined into an area-weighted average based on the spatial coverage of hummocks versus hollows as described above. Data for shrub coarse-root biomass (diameter > 2 mm) was based on harvests of the surface peat layer performed on ambient 1.13 m^2 quadrats in 2017 ($n=6$; Table 1; raw data in Supplemental Table 2). Aboveground, we found that annual production of new stems was 20% of the aboveground stem biomass pool (Hanson et al. 2018b data citation). To calculate shrub coarse-root production, we assumed annual belowground coarse root production similarly made up 20% of the belowground coarse root pool. Coarse roots of ericaceous shrubs are generally considered structural tissues, similar to aboveground stems (Klimešová et al. 2018), so we felt this assumption was justified. Elemental content of understory aboveground biomass and production was calculated based on %N analysis of tissues from the 2012, 2017, and 2018 understory harvests. %P data were from the compiled plant tissue chemistry dataset described above and in Table 1. Calculations regarding understory fine-root biomass and productivity are detailed below.

Fine root biomass and production

Biomass of fine roots (< 2 mm diameter) at the S1 Bog was reported by Iversen et al. (2018a). Fine-root biomass of hummocks and hollows was determined by sorting fine roots from a subset of the 2012 peat cores described above. Roots from *Picea*, *Larix*, shrubs, and graminoids were identified and separated. Live roots were differentiated from dead roots based on ^{14}C age and were found exclusively within the acrotelm [0–30 cm; see Iversen et al. (2018a)]. Fine-root biomass pools from hummocks and hollows were combined into an area-weighted average as described above.

Fine-root production was measured at the S1 Bog using both minirhizotrons and ingrowth cores. Minirhizotron images were collected weekly at sampling locations across the S1 Bog from 2011–2012, as described in Iversen et al. (2018a). Tree, shrub, and sedge fine roots were differentiated visually, and productivity was calculated based on the appearance

and elongation of fine roots through time. Production of fine roots was scaled to g m^{-2} ground area based on relationships between specific root length (m g^{-1}) and root diameter for each PFT. We assumed a 2-mm image depth of view in these calculations (Johnson et al. 2001). Ingrowth cores have been deployed at S1 Bog since 2013 and provide a measure of root production within root-free peat (Iversen et al. 2018a, 2021; Malhotra et al. 2020a, b data citation). We considered the sampling locations where paired hummock and hollow minirhizotron tubes were installed to be spatial replicates for observations made prior to the delineation of SPRUCE plots (Table 1). Across these datasets, extreme heterogeneity in fine-root production was observed. Mean rates of production across years, methods, and microtopographic features often differed by orders of magnitude and had standard deviations greater than the mean (mean values ranged from 9–75 $\text{g dry weight m}^{-2} \text{ year}^{-1}$, standard deviations ranged from 23–134 $\text{g dry weight m}^{-2} \text{ year}^{-1}$). There were no discernable patterns for hummocks versus hollows, across the two methods, or between years. We therefore included both methods in our analysis to capture as much variation as possible. Fine-root production measured by minirhizotrons and ingrowth cores in hummocks and hollows was averaged across years and combined into area-weighted averages based on spatial coverage of hummocks versus hollows.

Tissues from newly-grown *Picea*, *Larix*, shrub and graminoid fine roots in ingrowth cores (Malhotra et al. 2020a, b) as well as S1 Bog voucher specimens (Iversen et al. 2021 data citation) were analyzed for %N and %P. Due to insufficient amounts of graminoid root tissue from the S1 Bog, we used %P data from graminoid roots in FRED 2.0, the Fine Root Ecology Database (Iversen et al. 2018a data citation; <https://roots.ornl.gov/>). FRED was filtered for live graminoid roots growing above 45° N latitude. Average %N and %P of fine roots from trees, shrubs, and graminoids were multiplied by fine-root biomass and production to calculate pools and fluxes of fine root N and P.

Sphagnum production

Measurements of *Sphagnum* production at the S1 Bog are detailed in Norby et al. (2019) and Norby et al. (2018 data citation). Briefly, a patch of *Sphagnum* stems trimmed to 7-cm length was placed in a mesh

column with a diameter of 38 mm. Columns were inserted in the bog in October to maintain close connection with the surrounding *Sphagnum* community. The columns were deployed for 1 year, after which the mass of new *Sphagnum* (beyond the initial 7-cm segment deployed) was measured. Dry matter increment from the columns was scaled up to whole plot ($\text{g m}^{-2} \text{ year}^{-1}$) based on surveys of percent fractional cover of *Sphagnum*. The %N and %P of *Sphagnum* tissues were measured in September of 2017 (Norby et al. 2020 data citation).

Interannual nutrient resorption and mobilization

Resorption of N and P (N_{RESORP} and P_{RESORP}) during the senescence of plant leaves was calculated at S1 Bog based on resorption efficiencies reported in the literature and the assumptions that leaf biomass pools were at steady state over the measurement period. Resorption efficiencies for vascular plant species at Mer Bleue Bog (Ontario, Canada) and Roseau County (Minnesota, USA) were averaged per PFT (Supplemental Table 3; Bares and Wali 1979; Wang et al. 2014a, b). In *Sphagnum* moss, nutrients are not translocated to a storage pool because growth occurs through continuous elongation of *Sphagnum* stems from the capitula. Nutrients in the capitula can either stay in place and be part of the newly elongated stem, or they can move vertically upward and be part of the new capitula (Aldous 2002a, b). A *Sphagnum* mobilization term, akin to vascular plant resorption efficiency, can therefore be calculated by comparing the nutrient content of capitula versus stems. *Sphagnum* capitula and stems were sampled in ambient plots in 2017 and 2018 and mobilization efficiency for N and P was calculated for each plot. Mobilization efficiency was then multiplied by *Sphagnum* annual production to get an annual flux of recycled nutrients within *Sphagnum* (N_{MOBILIZE} , P_{MOBILIZE}).

Porewater

The content of N and P in porewater at the S1 Bog is described in (Griffiths and Sebestyen 2016). Total N (TN) and Total P (TP; organic and inorganic species) were measured on porewater samples collected from piezometers at 6 depths per plot in 2011–2013. Porewater N and P concentrations were then converted to pools (g N or P m^{-2}) as described in Griffiths and

Sebestyen (2016). This calculation was based on the water-filled porosity of peat, which varied with depth. Pools from 0–2 m were considered in this analysis so that the depth of the porewater pool matched that of peat coring profiles.

Bulk deposition

Bulk deposition was collected at the S1 Bog following every precipitation event starting in 2013. The precipitation collector was placed in a gap in the canopy and sampled both wet and dry deposition. TN was multiplied by the volume of collected precipitation to calculate daily deposition (Sebestyen et al. 2020 data citation). Bulk deposition rates of TN measured at the S1 Bog were similar to wet plus dry deposition measured at EPA Castnet sites in Minnesota ($0.55 \text{ g N m}^{-2} \text{ year}^{-1}$ for 2000–2018; <https://www.epa.gov/castnet>). This similarity supports our assertion that the precipitation collector at the S1 Bog captured dry as well as wet deposition. To quantify the flux of TP in deposition, we measured TP on samples from the precipitation collector. However, we found that 98% of measurements were below our detection limit of 0.05 mg P L^{-1} (Supplemental Fig. 1). We therefore decided to use low, high, and “regional” concentrations multiplied by S1 Bog’s precipitation volume to understand the potential range of TP in deposition. The low concentration considered was $0.010 \text{ mg P L}^{-1}$ and the high concentration was $0.075 \text{ mg P L}^{-1}$. The regional concentration was derived from 19 sites in the upper Midwest and Ontario and equaled $0.039 \text{ mg P L}^{-1}$ (Supplemental Table 4).

Lateral outflow

Enclosed plots at the SPRUCE experiment have underground corrals installed from just above the peat surface down to the mineral soil below (Sebestyen and Griffiths 2016 data citation). These corrals hydrologically isolate each plot from the surrounding bog and two slotted pipes installed horizontally at the peat surface as well as at 40 cm depth to allow natural drainage of water from the acrotelm to a reservoir outside each corral (Griffiths and Sebestyen 2016). At the reservoir, lateral outflow volume was quantified, and water was collected for chemical analysis (Sebestyen et al. 2021a, b data citation, Sebestyen et al. 2017 data citation). TN and TP concentrations

were measured on weekly composited, subsampled aliquots collected at 75-L volumetric intervals to accurately flow-weight outflow solutes. Ambient plots at SPRUCE do not have corrals installed, but the experimental SPRUCE plot maintained as a control for infrastructure installation, does. In addition to the belowground corral, this control plot has an aboveground enclosure and air blowing system but is not subjected to any warming or CO₂ treatment. Only lateral outflow measured at the control plot from 2017–2018 is included in this analysis to ensure ample time for the peatland system to recover from infrastructure installation (2012–2015).

Nitrogen fixation

Acetylene reduction assays (ARAs) have been used to quantify annual N fixation at MEF (S2 Bog, Urban and Eisenreich 1988) but this method underestimates fixation by methanotrophs in peatland bogs (Vile et al. 2014). ¹⁵N₂ tracers provide a more accurate representation of N fixation in these ecosystems and have been employed by Carrell et al. (2019) and Warren et al. (2017) at the S1 Bog. Carrell et al. (2019) data were based on 3 day incubations of freshly collected *Sphagnum* from the S1 Bog in 2017 (n=5 measurements from enclosed but unwarmed plots). These incubations took place in the lab at 25 °C and rates were consistent with incubations conducted over multiple seasons (Warren et al. 2017) as well recent in-situ measurements of *Sphagnum* tissue from 0–10 cm at S1 Bog (Petro et al. unpublished data). In the latter, *Sphagnum* tissues from 0–10 cm depths were incubated for several days in vials inserted into the *Sphagnum* layer. Research by Warren et al. (2017) also showed nitrogenase activity was relegated to the top 10 cm of *Sphagnum* at S1 Bog. Given the consistent rates of N fixation observed throughout the growing season and known depth of nitrogenase activity, we felt justified temporally and spatially scaling the N fixation rates from Carrell et al. (2019). Daily N fixation was scaled from g dry *Sphagnum* tissue to m² ground area based on the density of the top 10 cm of the *Sphagnum* layer (Norby and Childs 2018 data citation). Average daily temperatures measured at the *Sphagnum* surface were then calculated based on 2011–2013 pre-treatment environmental monitoring data (n=6 locations; Hanson et al. 2015 data citation). The Q₁₀ measured by Urban and Eisenreich in

the adjacent S2 Bog (ARA method, 3.1±1.3) was then used to temperature-correct daily N fixation for all days with average temperatures above freezing. The S2 Bog is a smaller, 3.2-ha ombrotrophic bog at the Marcell Experimental Forest with a similar pH and closed-canopy *Picea* overstory (Sebestyen et al. 2021a, b). Standard error (SE) associated with the reported annual N fixation rate was propagated from SE associated with the original N fixation rate reported by Carrell et al. (2019) as well as the error associated with Q₁₀ from Urban and Eisenreich (1988).

Denitrification and ammonia volatilization

To quantify gaseous losses of N, fluxes of N₂O and NH₃ were measured in the field at the S1 Bog (Bridgham raw data in Supplemental Fig. 2). Nine 40 cm-diameter collars were permanently installed outside of the SPRUCE plots with PVC covers. Fluxes of N₂O and NH₃ were measured in nine locations in S1 Bog over 2 days in September 2018 and 3 days in June 2019 (Bridgham, Supplemental Fig. 2). During measurements, a Gasetm DX4040 Fourier-transform infrared gas analyzer was connected to the chambers in a continuous closed-loop configuration for 10–60 min and concentrations were averaged every 30 or 60 s. Individual measurements were visually analyzed for the linear portion of fluxes. If the p-value of the increase in concentration over time was greater than 0.05, the flux was given a value of a zero. Although many flux rates were given a value of zero (9 of 22 measurements for N₂O, 16 of 21 for NH₃), detection levels for a significant flux were quite good (N₂O=0.9 nmole N m⁻² min⁻¹, NH₃=3.8 nmole N m⁻² min⁻¹). Measured rates for NH₃ averaged 0.002±0.001 μmole N m⁻² min⁻¹ but rates for N₂O were not distinguishable from zero and were frequently negative, indicating net consumption of N₂O (Supplemental Fig. 2). Given the fact that the measured N₂O fluxes spanned zero, we deemed it inappropriate to scale this rate up to an annual denitrification rate. We instead considered the range of observed denitrification reported by Urban et al. (1988) from the S2 Bog. They used acetylene inhibition methods with an in situ chamber to sample fluxes from unsaturated peat over a period of 24 h. The rates reported by Urban et al. ranged from 0.3–2.8 μg N m⁻² h⁻¹. To scale these rates from hourly to annual time periods,

we assumed the rate was applicable to the average snow-free period at the S1 Bog (234 days; Heiderman et al. 2018 data citation). The resulting rates ranged from 0.002 to 0.013 g N m⁻² year⁻¹, similar to annual rates generated from acetylene inhibition lab incubations for S2 Bog by Hill et al. (<0.001 to 0.020 g N m⁻² year⁻¹; 2016). Acetylene inhibition methods have been shown to underestimate denitrification in low-nitrate ecosystems like low-N bogs (Groffman et al. 2006; Sgouridis et al. 2016). However, the fact that field measurements of N₂O fluxes at the S1 Bog were indistinguishable from zero supports our assertion that denitrification is extremely low at this site. Field measurements of gaseous losses of NH₃ were positive (Supplemental Fig. 2) and were therefore scaled up to an annual rate based on the same 234-day snow-free period described above.

Modeling N & P in ELM-SPRUCE

We used ELM-SPRUCE, a version of the Energy Exascale Earth System Model (E3SM) land model (ELM) that was designed for simulating peatland ecosystems such as the SPRUCE site. ELM-SPRUCE includes ombrotrophic bog hydrology, hummock and hollow microtopography, and peat profile dynamics (ELM-SPRUCE; Shi et al. 2015; Griffiths et al. 2017). ELM-SPRUCE also includes C-N-P interactions and storage pools as well as site-specific parameterization of bog PFTs, including *Sphagnum* mosses, shrubs, evergreen needleleaf trees, and deciduous needleleaf trees (Shi et al. 2015, 2021; Yang et al. In prep). ELM-SPRUCE was parameterized using the observed N and P concentrations of leaves and assumed a 50% resorption rate for leaf litter for all PFTs (Yang et al. In prep; stoichiometric parameters listed in Supplemental Table 5). The model was spun up by continuously cycling the 2011–2017 meteorological forcing data from the weather station at the S1 Bog with preindustrial CO₂ concentrations and N deposition. The weather station was outside of the SPRUCE enclosures and therefore was not impacted by the experimental warming treatments that began in 2015. After spin-up, a historical transient simulation from 1850 through 2017 was run and model outputs from 2012–2017 were averaged. Modeled N and P pools and fluxes of trees (*Picea* versus *Larix*), *Sphagnum* mosses, and shrubs under ambient conditions are presented in this analysis. Together these PFTs

represented 99% of biomass and 93% of NPP at the S1 Bog (Tables 2 and 3).

Data analysis

N and P pool data were compiled from peat cores, porewater, and biomass at the S1 Bog to establish the distribution of N and P across this ecosystem. Within biomass data, the number of replicates differed for tissues and for understory plants, trees, and *Sphagnum* mosses (Table 1). In our initial analysis of ecosystem N and P pools, we considered tissue-specific pools of N and P in plant biomass so that the variation around mean could be directly assessed. To explore vegetation nutrient dynamics more fully, whole-plant pools of N and P were calculated for each PFT. For above-ground biomass and coarse tree roots, the number of plots measured was high (n = 16 to 21). Coarse shrub roots and fine roots of all PFTs, however, were measured at fewer locations (n = 3 to 6). Observations of above- and belowground tissues were not collected at the exact same locations or on the same spatial scale. As a result, average biomass values for coarse shrub roots and fine roots were added to plot-level pools of aboveground tissues and tree coarse roots to get whole-plant N and P pools. Variation around the mean therefore reflects variation in aboveground tissues and tree coarse roots.

N and P required for production of new biomass are referred to as N_{REQ} and P_{REQ} in this analysis and were calculated as the sum of N and P in annually-produced tissues for each PFT. Similar to the calculations of whole-plant biomass N and P, N_{REQ} and P_{REQ} included cross-plot averages for fine-root productivity. Coefficients of variation for whole-plant N and P pools as well as N_{REQ} and P_{REQ} therefore included spatial heterogeneity of aboveground biomass and coarse tree roots but did not include spatial variation of shrub coarse roots or fine roots of trees or shrubs.

To enable an estimate of annual N and P cycles for the S1 Bog, we assumed biomass at the S1 Bog was relatively stable during the measurement period (roughly 2009–2018). Though the S1 Bog does represent a regrowth stand, we assumed that the rapid regrowth period had ended (see Site Description). Biomass pools were assumed to be constant through time and we calculated annual N and P uptake (N_{UPTAKE}, P_{UPTAKE}) for each vascular PFTs based on the following equations:

Table 2 Ecosystem pools of N and P in peat, biomass, and porewater

Ecosystem component	n =	N pool (g N m ⁻² ± SE)	P pool (g P m ⁻² ± SE)	N PoolSpatial CV (%)	P PoolSpatial CV (%)
Peat					
Catotelm (80–200 cm)	16	4604 ± 134 ^A	127 ± 10 ^A	11.62	29.76
Mesotelm (30–80 cm)	16	1903 ± 115 ^B	56.22 ± 3.93 ^B	24.12	27.93
Acrotelm (0–30 cm)	16	337 ± 57 ^C	17.13 ± 2.24 ^C	68.10	52.37
Porewater	16	0.60 ± 0.04 ^J	0.05 ± 0.00 ^I	26.31	42.47
Biomass					
Sphagnum	16	29.24 ± 1.98 ^D	1.95 ± 0.14 ^D	27.02	27.89
Tree bole	21	5.61 ± 0.56 ^E	0.66 ± 0.07 ^E	45.76	45.73
Tree branch	21	3.88 ± 0.39 ^{EF}	0.45 ± 0.05 ^{EF}	45.81	45.77
Tree leaf	21	2.93 ± 0.30 ^{FG}	0.26 ± 0.03 ^G	46.47	47.41
Tree fine root	3	2.11 ± 0.63 ^{FGH}	0.24 ± 0.07 ^{FGH}	51.37	50.65
Tree coarse root	21	1.22 ± 0.08 ^{HI}	0.14 ± 0.01 ^H	29.01	28.77
Understory leaf	17	3.15 ± 0.19 ^{FG}	0.20 ± 0.01 ^{GH}	24.59	25.20
Understory fine root	3	2.37 ± 0.48 ^{EF}	0.21 ± 0.04 ^{FGH}	35.40	35.40
Understory stem	17	2.26 ± 0.25 ^G	0.19 ± 0.02 ^{GH}	46.24	42.70
Understory coarse root	6	0.63 ± 0.07 ^{IJ}	0.06 ± 0.01 ^I	25.70	25.70
Peat total		6845 ± 185	200 ± 10		
Biomass total		51.68 ± 2.28	4.23 ± 0.18		
Tree total		15.75 ± 0.98	1.76 ± 0.11		
Understory total		8.42 ± 0.58	0.66 ± 0.05		
Ecosystem total		6897 ± 185	204 ± 10		
Tree ratio of above: below		3.72 ± 0.74	3.62 ± 0.70		
Understory vascular plant above: below		1.80 ± 0.31	1.49 ± 0.26		
Total vascular plant above: below		2.81 ± 0.38	2.74 ± 0.37		

Means are presented ± standard error based on spatial (but not temporal) replicates. Values over 100 g m⁻² were rounded to the nearest whole number. Different letters within groups denote significant differences across pools for either N or P. Significance is based on estimated marginal means and $\alpha=0.05$

$$N_{\text{UPTAKE}} = N_{\text{REQ}} - N_{\text{RESORP}}$$

$$P_{\text{UPTAKE}} = P_{\text{REQ}} - P_{\text{RESORP}}$$

These equations assumed that all nutrients resorbed during senescence were mobilized for new growth in the following year. For *Sphagnum*, N_{RESORP} and P_{RESORP} were replaced by N_{MOBILIZE} and P_{MOBILIZE} in the equations above (see *Interannual Nutrient Resorption and Mobilization* above). For all PFTs, mean residence time (in years) for N and P was calculated as:

$$N_{\text{RESIDENCETIME}} = \frac{\text{BiomassN}}{N_{\text{UPTAKE}}}$$

$$P_{\text{RESIDENCETIME}} = \frac{\text{BiomassP}}{P_{\text{UPTAKE}}}$$

Biomass N and P as well as N_{REQ} and P_{REQ} from the empirical dataset were compared to model output from ELM-SPRUCE. ELM-SPRUCE represented deciduous and evergreen trees with separate PFTs, so data for *Larix* and *Picea* species were presented separately in this analysis. Rates of tree fine-root production were not separated by species in Iversen et al. (2018a; b), so we assumed the ratio of *Larix* to *Picea* fine-root production matched that seen in *Larix* and *Picea* fine-root biomass pools. Modeled versus field data were fit with linear models with free intercepts to assess correlations between field observations and ELM-SPRUCE output.

Table 3 N and P in plant functional types (PFTs) at the S1 Bog

	Biomass N			N _{REQ}			N _{RESORP}			N _{RESORP}			N _{UPTAKE}			N _{RESIDENCE TIME}		
	n	Mean ± SE (g N m ⁻²)	CV (%)	n	Mean ± SE (g N m ⁻² year ⁻¹)	CV (%)	n	Mean ± SE (g N m ⁻² year ⁻¹)	CV (%)	n	Mean ± SE (% of N _{REQ})	CV (%)	n	Mean ± SE (g N m ⁻² year ⁻¹)	CV (%)	n	Mean ± SE (year)	CV (%)
Sphagnum	16	29.24 ± 1.98 ^A	27.02	2	4.65 ± 2.30 ^{AB}	69.87	2	1.55 ± 0.86 ^{AB*}	78.47	2	32.04 ± 2.68 ^{AB*}	11.84	2	3.10 ± 1.44 ^{AB}	65.57	2	13.94 ± 8.16 ^{ABC}	82.78
Tree	21	15.77 ± 1.29 ^{AB}	37.42	21	2.60 ± 0.16 ^A	28.14	21	0.73 ± 0.08 ^A	49.15	21	26.87 ± 1.52 ^{AB}	25.85	21	1.86 ± 0.09 ^A	21.8	21	8.31 ± 0.45 ^{AB}	25.07
Shrub	17	6.85 ± 0.34 ^{BC}	20.48	17	2.70 ± 0.16 ^A	24.54	17	0.65 ± 0.04 ^A	28.43	17	23.76 ± 0.29 ^A	5.1	17	2.05 ± 0.12 ^A	23.33	17	3.37 ± 0.08 ^B	9.42
Sedge	17	0.34 ± 0.05 ^{CD}	59.79	17	0.46 ± 0.05 ^{BC}	44.57	17	0.17 ± 0.03 ^{BC}	60.86	17	33.51 ± 2.11 ^B	25.94	17	0.29 ± 0.03 ^{BC}	35.22	17	1.06 ± 0.08 ^{CD}	31.29
Forb	17	0.27 ± 0.03 ^D	51.84	17	0.27 ± 0.03 ^C	51.84	17	0.01 ± 0.00 ^C	59.63	17	4.19 ± 0.50 ^C	49.05	17	0.25 ± 0.03 ^C	51.01	17	1.05 ± 0.00 ^D	0
	Biomass P			P _{REQ}			P _{RESORP}			P _{RESORP}			P _{UPTAKE}			P _{RESIDENCE TIME}		
n	Mean ± SE (g P m ⁻²)	CV (%)	n	Mean ± SE (g P m ⁻² year ⁻¹)	CV (%)	n	Mean ± SE (g P m ⁻² year ⁻¹)	CV (%)	n	Mean ± SE (% of P _{REQ})	CV (%)	n	Mean ± SE (g P m ⁻² year ⁻¹)	CV (%)	n	Mean ± SE (year)	CV (%)	
Sphagnum	16	1.95 ± 0.14 ^A	27.89	2	0.35 ± 0.12 ^{AB}	46.87	2	0.13 ± 0.05 ^{AB*}	58.23	2	35.34 ± 3.29 ^{AB*}	13.16	2	0.22 ± 0.06 ^{AB}	40.36	2	12.06 ± 4.80 ^A	56.25
Tree	21	1.76 ± 0.14 ^A	37.3	21	0.26 ± 0.01 ^A	25.68	21	0.04 ± 0.00 ^A	54.79	21	13.49 ± 1.09 ^B	36.88	21	0.23 ± 0.01 ^A	22.92	21	7.65 ± 0.38 ^A	22.6
Shrub	17	0.56 ± 0.03 ^B	18.44	17	0.20 ± 0.01 ^A	23.51	17	0.03 ± 0.00 ^A	28.43	17	15.20 ± 0.24 ^B	6.45	17	0.17 ± 0.01 ^A	22.73	17	3.44 ± 0.08 ^A	9.28
Sedge	17	0.03 ± 0.00 ^{BC}	56.36	17	0.03 ± 0.00 ^{BC}	43.61	17	0.01 ± 0.00 ^{BC}	56.46	17	36.87 ± 2.05 ^A	22.88	17	0.02 ± 0.00 ^{BC}	34.59	17	1.16 ± 0.08 ^B	29.78
Forb	17	0.01 ± 0.00 ^C	54.83	17	0.01 ± 0.00 ^C	54.83	17	0.00 ± 0.00 ^C	63.7	17	12.29 ± 1.50 ^B	50.22	17	0.01 ± 0.00 ^C	53.76	17	1.19 ± 0.00 ^B	0.4

Means are presented ± standard error based on spatial (but not temporal) replicates. N_{REQ} and P_{REQ} are annual fluxes of N and P in production of new biomass. N_{RESORP} and P_{RESORP} are the N and P resorbed from leaves during senescence. For *Sphagnum*, we calculated this as N_{MOBILIZE} and P_{MOBILIZE} based on the difference between nutrient concentrations in old and new growth (values marked with asterisk). N_{UPTAKE} and P_{UPTAKE} are estimated uptake of N and P from soil (nutrient requirement minus resorption). Residence time is the biomass pool divided by uptake rate for each nutrient. Superscript letters indicate statistically significant differences between PFTs based on Kruskal–Wallis rank sums ($\alpha=0.05$). There was a small pool of unidentified plant species not included in PFT-level analysis but are in Table 2 pools (<0.2% of total biomass)

All graphing and statistics were performed in R version 4.0.0 (R Core Team 2020). For ecosystem pools of N and P as well as vegetation pools and fluxes, multiple years of data were available for only a few variables, notably aboveground biomass and production. In these instances, pools and fluxes per plot were calculated as the average across years. Spatial, but not temporal, variation was therefore considered. The coefficient of variation (CV) across spatial replicates was then calculated as the standard deviation divided by the mean and was expressed as a percent ($\times 100$).

For bulk deposition and lateral outflow of N and P at the S1 Bog, measurements were not spatially replicated but did take place over several years. For these fluxes, we therefore took into account temporal but not spatial variation. Standard error associated with these fluxes was calculated using years as replicate observations. Net annual fluxes of N and P were calculated by summing annual inputs and outputs from the ecosystem and propagating error associated with this sum. To understand the seasonal patterns driving annual budgets of N and P, we looked at cumulative daily deposition, outflow, and N fixation. Cumulative daily deposition and outflow data were from 2017–2018 only since these were the only years of overlapping data. Cumulative daily N fixation rates were described above (see *Nitrogen Fixation*).

To compare the size of ecosystem N and P pools, one-way analysis of variance (ANOVA) was performed on log transformed data to improve normality. Marginal means from this ANOVA model were then estimated for each pool or flux and compared based on Tukey comparisons with $\alpha=0.05$ (*emmeans* package). Estimated marginal means take into account unbalanced sample design by calculating unweighted averages across pools (Searle et al. 1980). When investigating nutrients in biomass, production, resorption, and uptake across PFTs, we opted to use a non-parametric test due to non-normal distribution of the data. We performed Kruskal–Wallis rank sums along with a post-hoc Dunn test based on Bonferroni adjusted p-values for comparisons between groups.

To understand the relative importance of N and P in the S1 Bog ecosystem, we looked at the mass-based ratio of N to P (N:P) within plant biomass. This ratio can indicate whether N or P is limiting key biological processes within the plant, but there are limitations to inference one can draw from N:P since

this ratio can vary with age, tissue, and growth form (Güsewell 2004). N:P of whole plants can, however, be used as a relative metric for the nutrient status of plants, with lower values indicating a greater scarcity of N compared to plant demand and higher values indicating a greater scarcity of P compared to plant demand. In wetland plants, N:P mass-based ratios over 16 has been shown to signify P limitation, while N:P under 14 signifies N limitation (Koerselman and Meuleman 1996; Güsewell and Koerselman 2002). These values, however, should be considered broad indicators along the spectrum of N to P limitation rather than absolute thresholds. We compared the N:P in plant biomass and $N_{REQ}:P_{REQ}$ across PFTs using estimated marginal means.

Results

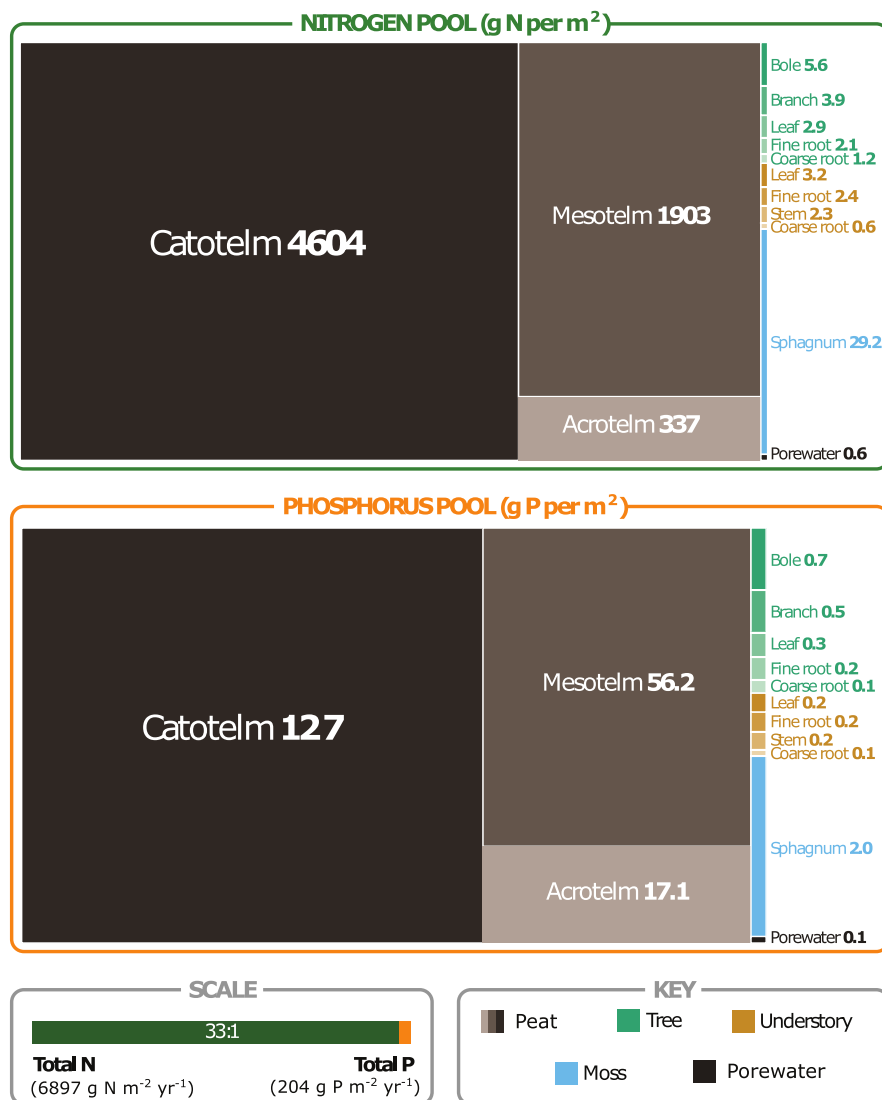
Pools of N and P

Analysis of the various ecosystem N and P pools showed that the peat stored an overwhelming majority of these two nutrients in S1 Bog (Fig. 1, Table 2). Peat stored 6845 ± 185 g N m⁻² which was $99.2 \pm 3.8\%$ of ecosystem N. P in peat was a smaller pool (200 ± 10 g m⁻²) but made up a similar percentage of ecosystem P ($97.9 \pm 7.2\%$). Peat at the S1 Bog had an overall N:P ratio of 34.2 ± 2.0 , and the spatial coefficient of variation (i.e., CV) of peat N and P was lower in the catotelm than in the acrotelm (Table 2).

Among the plant components of the ecosystem, *Sphagnum* stored 29.2 ± 2.0 g N m⁻² and 2.0 ± 0.1 g P m⁻². These pools made up close to half of vegetation biomass N and P for the whole ecosystem ($54.8 \pm 4.4\%$ and $44.6 \pm 3.7\%$, respectively). The *Sphagnum* N pool was almost twice as large as the tree N pool (29.2 ± 2.0 versus 15.8 ± 1.0 g N m⁻², p value < 0.001). Phosphorus, on the other hand, was more evenly distributed between *Sphagnum* and trees (*Sphagnum* 2.0 ± 0.1 g P m⁻², tree 1.8 ± 0.1 g P m⁻²). Interestingly, the spatial CV of *Sphagnum* N and P was also low compared to the acrotelm (Table 2). For both N and P, understory plants stored about 15% of the total biomass nutrient pools ($15.8 \pm 1.3\%$ biomass N, and $15.2 \pm 1.3\%$ biomass P).

The fine-root N pool of trees was similar in size to leaf N pools (2.1 ± 0.6 g N m⁻² versus 2.9 ± 0.3 g N m⁻²). P pools in tree fine roots and

Fig. 1 N and P pools across biotic and abiotic components of the S1 Bog ecosystem. Area of the boxes for each N and P pool reflect pool sizes. Note the different scales used to depict storage of these two nutrients: the total ecosystem N pool is 33× larger than the ecosystem P pool



leaves were also similar in size (0.2 ± 0.1 g P m⁻² versus 0.3 ± 0.0 g P m⁻²). In understory plants, which include shrubs, sedges, graminoids and forbs, fine roots stored more N than coarse roots (2.4 ± 0.5 g N m⁻² versus 0.6 ± 0.1 g N m⁻²; p value=0.001) and stored a similar amount of N as stems (2.3 ± 0.3 g N m⁻²). Phosphorus in understory plants had a similar distribution, with fine roots storing more P than coarse roots (0.2 g P m⁻² versus 0.1 g P m⁻²; p value=0.001) and a similar amount to stems (0.2 g P m⁻²).

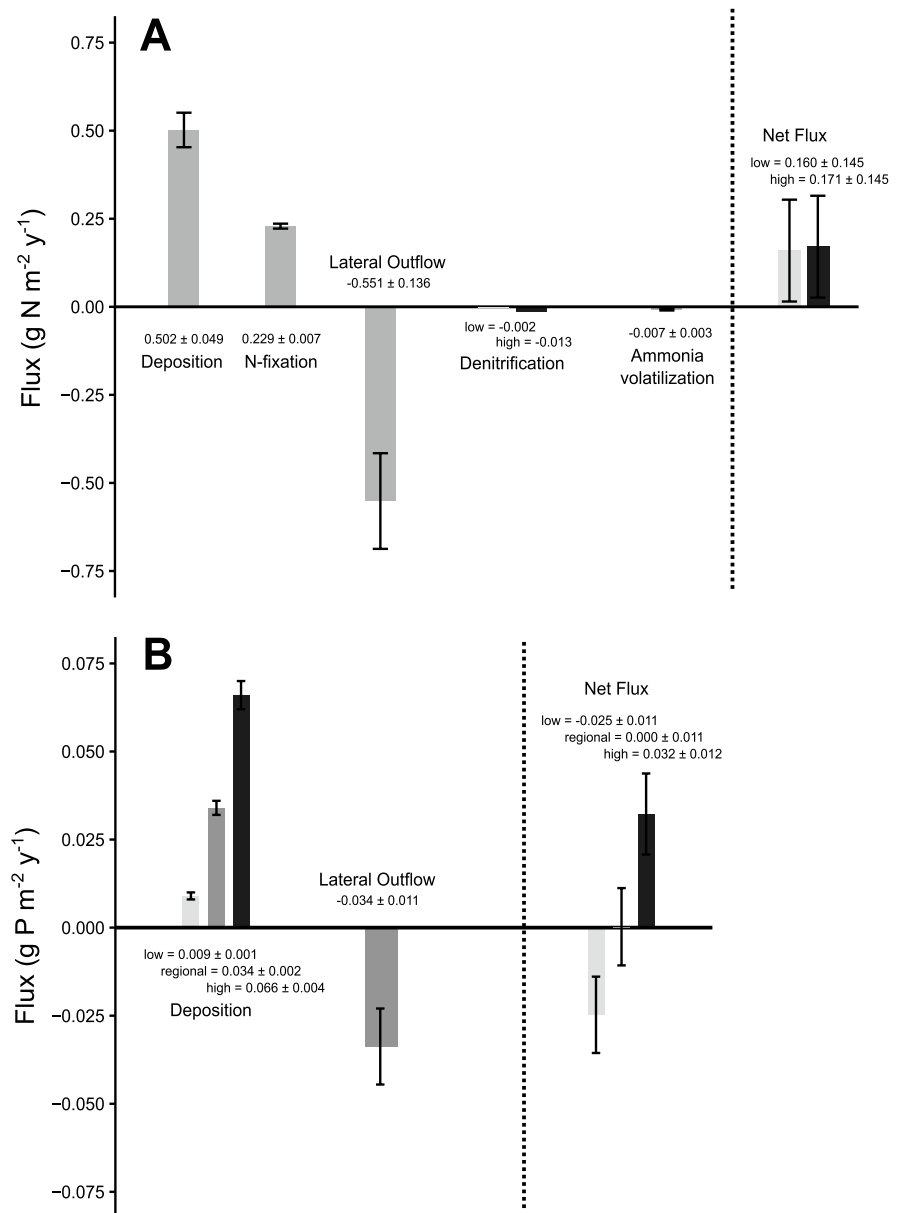
At S1 Bog, understory plants stored proportionally more N and P belowground than trees did (Table 2; Fig. 1). Above-to-belowground ratios of biomass N

were 1.8 ± 0.3 for the understory and 3.7 ± 0.7 for trees (p value < 0.001). Above-to-belowground ratios of biomass P mirrored this pattern with 1.5 ± 0.3 for understory and 3.6 ± 0.7 for trees (p value < 0.001).

Ecosystem fluxes: annual versus seasonal balance

Annual fluxes for N and P into and out of the S1 Bog indicate that the ecosystem is a slight sink for N but is neither accumulating nor losing P (Fig. 2). Nitrogen inputs included both deposition as well as N fixation, with the latter making up about one-third of total N inputs to the ecosystem. N losses included lateral outflow, denitrification,

Fig. 2 Annual fluxes of nitrogen (A) and phosphorus (B) entering and leaving the S1 Bog. Error bars represent standard error. Positive values represent inputs while negative values represent losses from the ecosystem and net fluxes were calculated as the sum of all inputs and losses. In (A), high and low net fluxes included high versus low denitrification. In (B), high, best, and low net fluxes included high, regional, or low rates of deposition, respectively



and ammonia volatilization and were driven almost exclusively by lateral outflow. The annual net flux of N accumulating in the S1 Bog ecosystem was $0.2 \pm 0.1 \text{ g N m}^{-2} \text{ year}^{-1}$ whether high or low rates of denitrification were considered (Fig. 2A). Denitrification reported in our study was based on rates reported in Urban et al. (1988) and were lower than annual rates in Urban and Eisenreich (1988; $0.18 \text{ g N m}^{-2} \text{ year}^{-1}$). This difference is likely because Urban and Eisenreich's rate was characterized as potential denitrification based on total

nitrate in throughfall at the S2 Bog rather than actual measurements.

Our best estimate of P deposition based on reported TP concentrations in the region was $0.03 \text{ g P m}^{-2} \text{ year}^{-1}$ but it is possible this rate could be as low as 0.01 or as high as $0.07 \text{ g P m}^{-2} \text{ year}^{-1}$ based on range of concentrations in samples from S1 Bog (Fig. 2B, See *Bulk Deposition* and Supplemental Table 4). If the regional estimate for P deposition is considered, the net flux of P at the S1 Bog is zero and the ecosystem is neither a sink nor a source for P. If

the low or high-end estimates of P deposition are considered, the ecosystem is either losing or gaining P at $0.03 \text{ g P m}^{-2} \text{ year}^{-1}$. Given the fact that precipitation samples collected at S1 Bog were near or below the detection limit, however, we do not consider the high or low-end rates of P deposition to be plausible. They do, however, provide important context for the literature-derived regional estimate and assure us that this rate is within the range of expected values for the S1 Bog.

Though the net annual fluxes of both N and P were low, there were seasonal differences in the cumulative daily fluxes of these two nutrients (Fig. 3). During the snow-covered periods of the year, N in atmospheric deposition was greater than N lost in lateral outflow, and thus N tended to accumulate in the ecosystem (Fig. 3A). Following snow melt, some N was transported downstream via lateral outflow, but N continued to accumulate in the ecosystem, especially in the late growing season. The seasonal dynamics of N accumulation were due in part to contributions of N fixation, which were greatest during the peak growing season when temperatures were highest. During fall senescence, N losses dominated until snow cover returned. The seasonality of P fluxes, in contrast, did not include a strong springtime accumulation (Fig. 3B). Instead, accumulation of P took place early in the year during snow-cover as well as late in the growing season.

Relative N and P across plant functional types

At the S1 Bog, the N:P of PFTs varied from 9 to 29 (Fig. 4). Forbs had the highest N:P, followed by the *Sphagnum* layer. Sedges and shrubs had a lower N:P than *Sphagnum* and the lowest N:P was seen in trees. Across all PFTs, the N:P of plant biomass at the S1 Bog was approximately 12.

N_{REQ} and P_{REQ} were defined as the nutrients in annually-produced plant tissues and totaled $10.7 \pm 2.3 \text{ g N m}^{-2} \text{ y}^{-1}$ and $0.9 \pm 0.1 \text{ g P m}^{-2} \text{ y}^{-1}$ at the S1 Bog (Table 3). *Sphagnum*, trees, and shrubs had statistically indistinguishable N_{REQ} and P_{REQ} fluxes (Table 3, Fig. 5). We observed very high spatial variation in *Sphagnum* N_{REQ} and P_{REQ} (CVs of 69.9% and 46.9% respectively, compared with 28.1% and 25.7% for tree N_{REQ} and P_{REQ}). Trees had the lowest ratio of N_{REQ} to P_{REQ} ; *Sphagnum*, shrubs, and sedges had intermediate values; and forbs had the highest

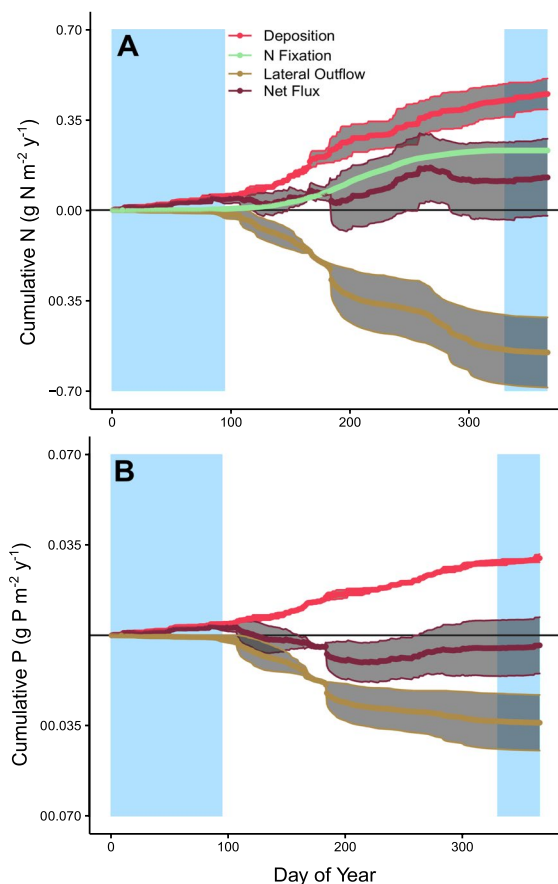


Fig. 3 Average daily cumulative fluxes of nitrogen (**A**) and phosphorus (**B**) in deposition, fixation, and lateral outflow at the S1 Bog. Grey shaded regions around lines represent the standard error calculated based on interannual variation in cumulative daily fluxes. P deposition rates were calculated based on regional values for total phosphorus concentrations (Fig. 2). Denitrification and ammonia emissions are not pictured. Rectangles shaded in blue denote the typical snow-covered period of the year

ratio (Fig. 5). Across PFTs, the ratio of N_{REQ} to P_{REQ} was significantly higher than the N:P of whole-plant biomass (paired two tailed t-test, p value < 0.001).

N_{REQ} and P_{REQ} were met by a combination of nutrients resorbed from leaves during senescence (N_{RESORP} and P_{RESORP}) and uptake of nutrients (N_{UPTAKE} and P_{UPTAKE}). When comparing PFTs, N_{RESORP} of *Sphagnum*, trees, and shrubs were similar in magnitude (1.6 ± 0.9 , 0.7 ± 0.1 , and $0.7 \pm 0.0 \text{ g N m}^{-2} \text{ year}^{-1}$ respectively). These three PFTs also had comparable P_{RESORP} (Table 3). Forbs and sedges had the lowest N_{RESORP} and P_{RESORP} fluxes, though for sedges,

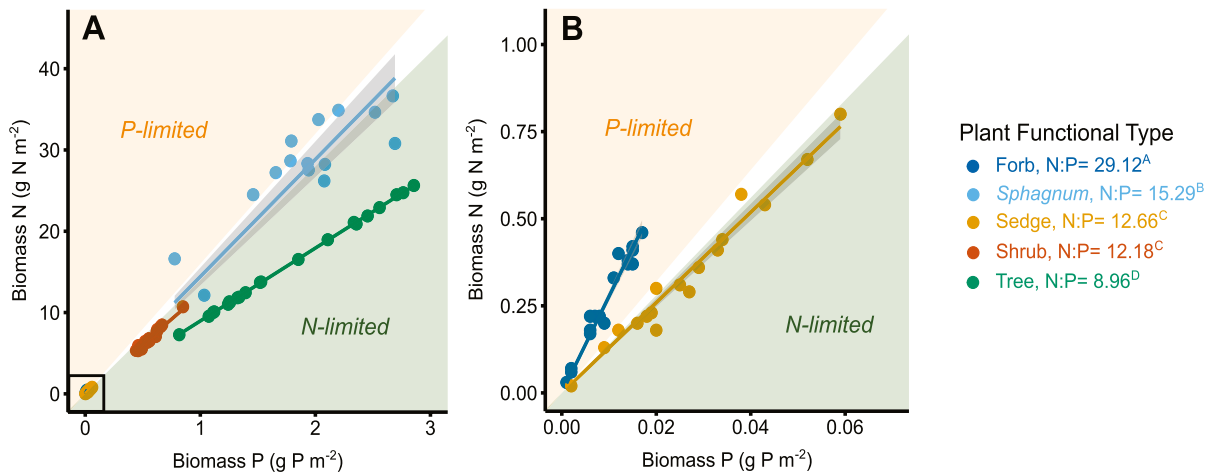
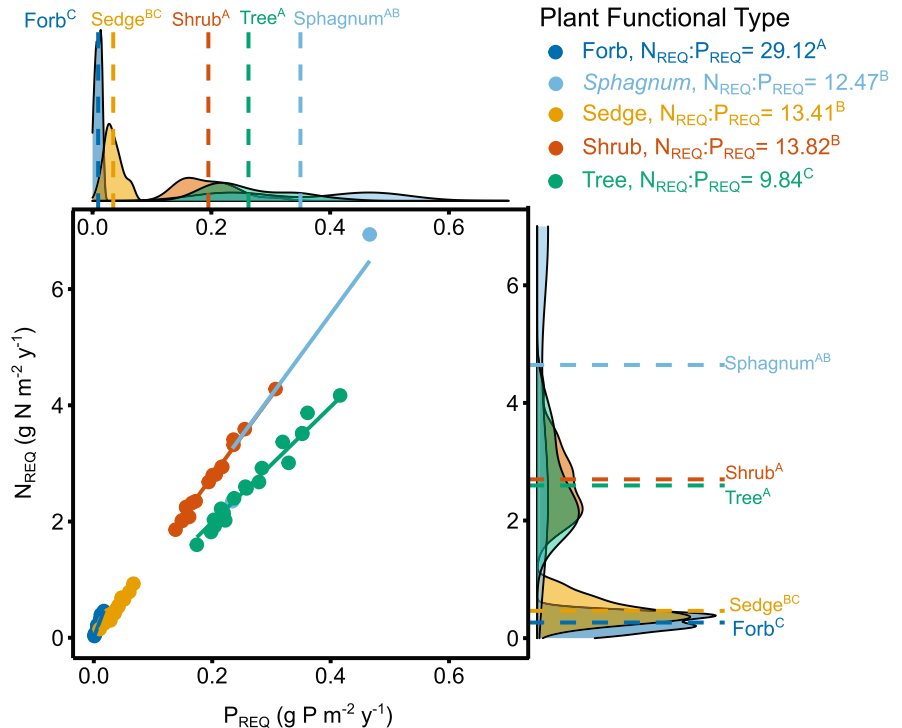


Fig. 4 Whole-plant biomass N versus P by plant functional type. Panel **B** is a re-scaled view of the area within the black box outlined in panel **A**. In both **A** and **B**, points represent plot-level observations and the orange area highlighted as “P limited” corresponds to N:P ratios of over 16 while the green

area highlighted as “N-limited” corresponds to N:P ratios under 14 (see “Methods”). Different superscript letters in the legend denote significant differences between plant functional type N:P ratios based on estimated marginal means ($\alpha < 0.05$)

Fig. 5 N_{REQ} versus P_{REQ} across plant functional types. Each point represents plot-level observations of N and P in annual net primary productivity. Density plots for N_{REQ} and P_{REQ} depict mean values per functional type with dashed lines. Superscript letters in the color-coded legend at the top right denote significant differences between N:P ratios of plant functional types based on estimated marginal means ($\alpha < 0.05$). Different superscript letters on labels for the density plots denote significant differences in N_{REQ} and P_{REQ} based on Kruskal–Wallis rank sums ($\alpha = 0.05$)



these fluxes provided a greater proportion of N_{REQ} and P_{REQ} ($33.5 \pm 2.1\%$ of sedge N_{REQ} compared to $4.2 \pm 0.5\%$ of forb N_{REQ} ; $36.9 \pm 2.1\%$ of sedge P_{REQ} compared to $12.3 \pm 1.5\%$ of forb P_{REQ}). In trees,

shrubs, and *Sphagnum*, N_{RESORP} and P_{RESORP} supported a similar percentage of N_{REQ} and P_{REQ} fluxes (Table 3). In both trees and shrubs, N_{RESORP} provided a greater percent of N_{REQ} than P_{RESORP} provided for

P_{REQ} (paired t-tests, p values both <0.001). Across all PFTs, uptake made up a majority of N_{REQ} and P_{REQ} (70.7% of N_{REQ} and 76.5% of P_{REQ} ; Fig. 1). Similar to the pattern seen in N_{RESORP} and P_{RESORP} , fluxes of N_{UPTAKE} and P_{UPTAKE} were highest in *Sphagnum*, trees, and shrubs and lowest in sedges and forbs.

ACROSS vascular PFTs, $N_{RESIDENCE\ TIME}$ was higher than $P_{RESIDENCE\ TIME}$ (Table 3, paired two tailed t-tests, p value=0.02) but when *Sphagnum* was considered, this pattern was no longer statistically significant (p=0.06). For both elements, trees and shrubs had longer residence times than sedges and forbs (Table 3).

Comparison with ELM-SPRUCE

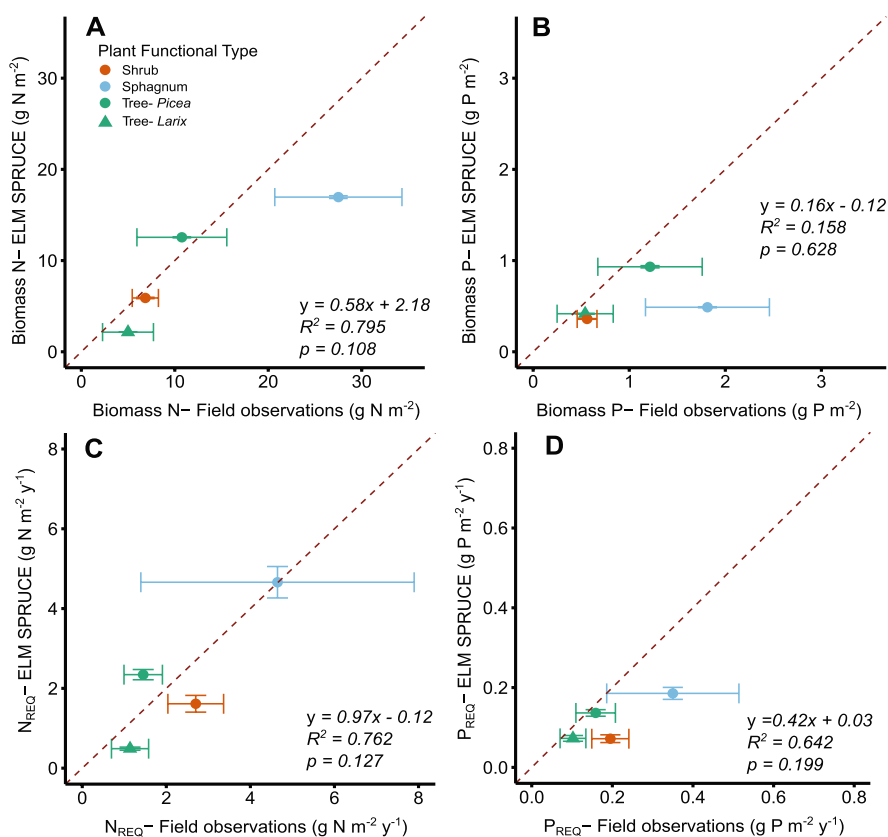
ELM-SPRUCE captured field observations of plant biomass N and N_{REQ} better than plant biomass P and P_{REQ} (Fig. 6). The model calculated partitioning of biomass N among the PFTs reasonably well ($R^2=0.80$, p value=0.11), though it underpredicted *Sphagnum* N. Modeled biomass P across PFTs did

not vary greatly and therefore did not portray the variation in biomass P observed in the field ($R^2=0.16$, p value=0.63). This poor fit was heavily influenced by the model's underestimation of *Sphagnum* P (Fig. 6B). When assessing the annually cycling of nutrients, the model captured field N_{REQ} better than field P_{REQ} (N_{REQ} $R^2=0.76$, p value=0.13; P_{REQ} $R^2=0.64$, p value=0.20). Similar to biomass P, modeled P_{REQ} did not capture the full range of P_{REQ} observed across PFTs in the field.

Discussion

In this analysis, nutrient budgets and stoichiometry from the ombrotrophic S1 Bog under ambient conditions were explored to better understand the ecosystem structure and function as well as the current representation of bog nutrient cycling within the land-component of an Earth System Model (ELM-SPRUCE). Our results emphasized the important role that peat played in storing N and P in this ecosystem

Fig. 6 Comparison between field data (x axes) and ELM-SPRUCE simulations (y axes) under ambient conditions. Biomass N (A), biomass P (B), N_{REQ} (C), and P_{REQ} (D) are presented for each plant functional type. Error bars associated with field observations represent standard errors around the mean based on spatial replicates and errors associated with model output represent interannual variation for 2012–2017. The 1:1 relationship is indicated with a dashed red line



and demonstrated that N was accumulating in the S1 Bog ecosystem at a rate of $0.2 \pm 0.1 \text{ g N m}^{-2} \text{ year}^{-1}$ but annual P inputs were likely balanced by losses. This accumulation rate is similar in size to annual inputs of N via N fixation within the *Sphagnum* moss layer. Plants varied in their relative degrees of N versus P limitation, internal recycling of N and P, and allocation of nutrients across tissues. Within the model ELM-SPRUCE, N pools and fluxes across PFTs were accurately simulated but the model tended to underestimate P pools and fluxes and was a poor match for field observations of *Sphagnum* biomass.

Nutrients in peat: peat dominates storage & N mineralization supplies two-thirds of N_{uptake}

Storage of N and P at the S1 Bog was driven by the large pools of these nutrients accumulated in peat. The N:P of peat increased from 18.4 ± 1.1 to 38.5 ± 2.2 when moving downward in the peat profile and was generally higher than the ratios seen in plant tissues (which ranged from 15.3 ± 0.7 in *Sphagnum* to 8.5 ± 0.0 in tree boles). The decreasing spatial variation seen in N:P from acrotelm to catotelm layers suggests that the decomposition stage of the peat in the upper layers is highly variable, potentially due to interactions with the water table depth or local litter inputs. Porewater, though a small pool of N and P, had an N:P of 13.6 ± 0.8 , similar to the N:P of understory plant tissues and *Sphagnum*. Microbial biomass N:P is likely around 3 at the S1 Bog (mass basis, Cleveland and Liptzin 2007; Wang et al. 2014a), much lower than the N:P of peat, plant tissues, and porewater at this site. Research at the S2 Bog by Hill et al. (2014) indicated P-limitation of microbial biomass which could be due to low P content of available substrates. Previous stoichiometric measurements associated with microbial enzyme activity in the S1 bog also suggested P and possibly N–P colimitations on microbial activity (Lin et al. 2014; Steinweg et al. 2018). However, more recent experimental incubations have indicated that pH and temperature constrain microbial decomposition more than N and P availability (Kluber et al. 2020).

The S1 Bog is a cold and nutrient-poor environment, so organic N is likely a significant source of N for plants (Schimel et al. 2004; Krab et al. 2008; Moore et al. 2018). In the present budget, plant reliance on organic N was not quantified directly but

we can estimate the size of this flux. N mineralization at S2 bog was approximately $5 \text{ g N m}^{-2} \text{ year}^{-1}$ (Urban and Eisenreich 1988) while total plant uptake of N at the S1 Bog was $7.6 \text{ g N m}^{-2} \text{ year}^{-1}$ and N fixation was $0.2 \text{ g N m}^{-2} \text{ year}^{-1}$ (Table 3; Fig. 2). Assuming the S2 Bog N mineralization rate applies to the S1 Bog, this would leave $2.4 \text{ g N m}^{-2} \text{ y}^{-1}$ difference between N mineralization and plant uptake that likely indicates the reliance of the plant community on organic N. Porewater N at the S1 Bog contained approximately 30% of organic N forms (Griffiths and Sebestyen 2016). The assumption that plants assimilate roughly one-third of their N from organic sources matches with observations of the pools of organic versus inorganic N in porewater. In other nutrient-poor ecosystems, partitioning of N forms amongst competing plants has been shown to match patterns of availability (McKane et al. 2002).

Though P mineralization has not been measured directly at MEF, ratios of N:P mineralization for anoxic versus oxic conditions have been reported for another Minnesota bog by Chapin et al. (2003). At the S2 Bog, roughly 64% of N mineralization came from the oxic peat (Urban and Eisenreich 1988). By multiplying the 10:1 ratio of N:P mineralization in oxic peat presented in Chapin et al. (2003) times 64% of the $5 \text{ g N m}^{-2} \text{ year}^{-1}$ mineralization rate from Urban and Eisenreich (1988), we estimated P mineralization in oxic peat at S1 Bog to be approximately $0.32 \text{ g P m}^{-2} \text{ year}^{-1}$. Performing the complementary calculation for anoxic peat mineralization using the 4:1 ratio of N:P mineralization in anoxic peat from Chapin et al. (2003), yielded P mineralization in anoxic peat rates of $0.45 \text{ g P m}^{-2} \text{ year}^{-1}$. Together, P mineralization in oxic and anoxic peat is therefore around $0.8 \text{ g P m}^{-2} \text{ year}^{-1}$. Total P_{UPTAKE} at the S1 Bog equaled $0.7 \pm 0.1 \text{ g P m}^{-2} \text{ year}^{-1}$ in this study. The similar sizes of estimated P mineralization rates and P_{UPTAKE} at the S1 Bog indicates that plant reliance on organic forms of P is likely low at this site.

Nutrient balance: N accumulates while P inputs roughly match P outputs

At the S1 Bog, we observed net accumulation of N but a neutral balance of P entering and exiting the ecosystem (Fig. 2). These inputs and outputs to the bog ecosystem were generally an order of magnitude smaller than the fluxes of N and P required

for plant NPP (Figs. 3, 5). Most of the N and P in this ombrotrophic bog was in peat, likely in biologically unavailable forms or deep in the soil profile. Thus, the efficient annual cycling of N and P through the ecosystem relies heavily on the cycling of these nutrients through trees, shrubs, *Sphagnum*, and near-surface peat layers.

Annual N dynamics show that deposition and fixation were greater than lateral outflow and gaseous N losses were so low that they had little impact on the annual N balance. The low rates of denitrification reported here (based on Urban and Eisenreich 1988) were consistent with the S2 Bog denitrification rates reported by Hill et al. (2016) as well as microbial genomic research at the S1 Bog that showed low relative abundance of potentially denitrifying bacteria (Lin et al. 2014). The rate of N accumulation at S1 Bog is slightly lower than range of N accumulation rates of other boreal ombrotrophic bogs ($0.5\text{--}4.8\text{ g N m}^{-2}\text{ year}^{-1}$, Moore et al. 2004). The temporal period over which accumulation rates are measured is important to take into account, however, and Moore et al. (2004) quantify accumulation over the last 150 years while this study presents a brief snapshot using data collected from 2010–2020. More broadly, the difference between the annual balance of fluxes of N and P at the S1 Bog prompts us to question why the P balance is near zero while N accumulates in the ecosystem when there is an abundance of PFTs that are co-limited by N and P (Figs. 2, 3). We suggest that this difference may be due to the peatland cycling a greater proportion of ecosystem P through plants and shallow soils. A higher proportion of ecosystem P was seen in plants and the acrotelm compared with N (Fig. 1). We also see that peat %P tends to decrease in the top of the profile while peat %N increases (Supplemental Fig. 3). Together, these observations suggest that the S1 Bog ecosystem retains P at the surface but buries N. Preferential mining of P by mycorrhizal fungi in surface soils could explain the stratified cycling of these two nutrients (Read et al. 2004). The mechanisms behind this stratified cycling of P deserve further investigation, especially since P cycling is relatively understudied compared to N cycling in peatlands.

Nutrients in plants: trees are the most N-limited PFT

The plant community at the S1 Bog appeared to be broadly co-limited by N and P, as has been observed in other ombrotrophic ecosystems (Iversen et al. 2010; Juutinen et al. 2010). However, the distinct N:P ratios observed across PFTs indicate that the degree of N versus P limitation varies for different plants (Fig. 4). This finding is similar to the constrained stoichiometry for bog shrubs, graminoids, forbs, and mosses at the Mer Bleue ombrotrophic bog in Ontario described by Wang et al. (2014a). In contrast to Mer Bleue, however, the S1 Bog is forested and our results show trees made up two-fifths of biomass and are the most N-limited PFT at this site. Shrubs at S1 Bog had a significantly higher N:P ratio and were more strongly limited by P than trees. The spatial variation of tree biomass N and P was greater than that of shrubs, likely due to the plot scale (66.4 m^2) of tree measurements versus the quadrat scale (0.25 m^2) of shrub measurements. At the quadrat scale, shrubs are relatively homogenous, but the open tree canopy at S1 Bog means trees are heterogenous across plots, ranging from 10–36 individuals per plot. *Picea* dominates the tree canopy at the S1 Bog but variable representation of *Larix* across plots likely added further spatial heterogeneity to tree biomass pools.

When assessing both nutrient storage and the annual fluxes of N and P in NPP at the S1 Bog, it is clear *Sphagnum* plays a pivotal role under ambient conditions. In addition to hosting N-fixing symbionts, N_{REQ} and P_{REQ} of *Sphagnum* are particularly large and highly variable (Fig. 5). There are only two data points for *Sphagnum* NPP in this current analysis, but each ambient plot observation is comprised of 2 years of data from three potential *Sphagnum* habitats (Norby et al. 2019). When converted to g dry mass, the rates in this present study are within the observed range from Canadian fen sites (Moore 1989) and the N:P ratio of *Sphagnum* is similar to what has been reported for other boreal bogs (Živković et al. 2017). Decreasing the assumed depth of the *Sphagnum* biomass pool from 10 to 6 cm to reflect only current-year *Sphagnum* tissues reduced the biomass pools to approximately 20.8 g N m^{-2} and 1.2 g P m^{-2} (Supplemental Appendix A).

Nutrients in models: N cycling in plants captured more accurately than P cycling

ELM-SPRUCÉ accurately portrayed N cycling within the dominant PFTs at the S1 Bog but the model underpredicted P and P_{REQ} and was notably low when it came to *Sphagnum* biomass N and P. The mismatch between modeled and measured *Sphagnum* biomass, however, can be fully explained by fact that the model assumed a 1-year residence time for *Sphagnum* while the empirical data included multi-year tissues in the *Sphagnum* biomass pool, resulting in longer residence times for *Sphagnum* N and P (“Methods”, Table 3). Modeled *Sphagnum* biomass pools were 17.0 g N m^{-2} and 0.5 g P m^{-2} and were quite close to the 1-year pools of *Sphagnum* biomass estimated above (20.8 g N m^{-2} and 1.2 g P m^{-2} ; Supplemental Appendix A). The model’s underprediction of *Sphagnum* N and P was primarily caused by differing assumptions about the definition of live *Sphagnum* biomass and the timeframe along which *Sphagnum* became part of the decomposing acrotelm. Since empirical studies vary in their delineation of live *Sphagnum*, this discrepancy is not unique to this study but should be considered when collecting field data for future model testing and parameterization.

The tendency for ELM-SPRUCÉ to underpredict biomass P is likely explained by N:P in the model being higher than observed values from the field. For trees, shrubs, and *Sphagnum* the model predicted N:P of 10.9, 16.4, and 34.8, respectively, which are all higher than the 9.0, 12.2, and 16.1 ratios observed in the field (Fig. 4). A higher N:P would explain the low modeled biomass P and P_{REQ} . If only one annual *Sphagnum* growth is considered, the field N:P of *Sphagnum* rose to 20, but was still lower than the N:P of modeled *Sphagnum* (34.8). This modeled *Sphagnum* N:P is also notably higher than the range reported by Aerts et al. (1999). This discrepancy can be partially attributed to the fact that stoichiometric parameters in ELM-SPRUCÉ were based on site-specific data for leaves, but wood and fine root parameters were set to default values (“Methods”, Supplemental Table 5). In the model, the default fine root N:P and wood N:P parameters were higher than the empirical data (Supplemental Table 5, Table 2), making vegetation more P-limited than observations would suggest. Storage pools of N and P within modeled PFTs also, however, had high N:P that also

inflated whole-plant N:P in the model. We therefore attribute the model’s high biomass N:P and underestimation biomass P and P_{REQ} to model parameterization with low N:P ratios for wood and fine-root stoichiometry well as inaccurate allocation of these nutrients to storage.

Ombrotrophic bog N and P cycling: insights into a warmer world

The N and P budget for the S1 Bog provides an important reference point for quantifying the impact of SPRUCÉ experimental treatments on nutrient cycling. Warming associated with climate change is expected to reduce C storage within peatland ecosystems by directly accelerating peat decomposition (Dorrepaal et al. 2009) and indirectly drying the peat profile (Alm et al. 1999; Bragazza et al. 2016). Across ecosystems, warming-induced increases in decomposition have a corresponding increase in N mineralization (Rustad et al. 2001). If N availability increases with warming at the S1 Bog, our results suggest that trees should benefit because they are more strongly N-limited than other PFTs at the S1 Bog (Fig. 4). Tree $N_{RESIDENCE \text{ TIME}}$ is quite long (8.3 ± 0.5 years), however, so trees may be slow to respond to such an increase in N availability (Table 3). Shrubs, which were shown to be more co-limited by N and P than trees (Fig. 4) and have a shorter $N_{RESIDENCE \text{ TIME}}$ than trees (3.4 ± 0.1 years), may respond more quickly. The shrub response could also be augmented if P mineralization is stimulated by concurrent drying of the peat profile (Bridgham et al. 1998). Increased shrub dominance under warmer and drier conditions has been demonstrated across ombrotrophic bogs along an altitudinal gradient (Bragazza et al. 2013) and was associated with a decrease in *Sphagnum*, an increase in soil fungi, and an increase in the contribution of organic N to total N availability (Bragazza et al. 2013, 2015).

Based on our analysis of N versus P cycling at the S1 Bog, a shift from *Sphagnum* to shrub dominance would increase belowground biomass allocation in this ecosystem and accelerate the N and P cycling through the biota due to the shrubs’ tendency to have shorter nutrient residence times and reduced reliance on resorbed N and P (Table 3). Interestingly, this presumption is already partially supported by observations from our first 4 years of manipulative warming

at SPRUCE. Across the manipulative warming treatments, there has been a decline in *Sphagnum* cover and productivity (Norby et al. 2019), an increase in shrub aboveground biomass and NPP (McPartland et al. 2020), and a proliferation of shrub fine-roots (Malhotra et al. 2020a, b). We therefore expect that available N and P in peat are increasing with warming. Plants at the S1 Bog appear to rely on organic N for about one third of their N uptake requirement, but this may change with warming due to the increase in ericaceous shrubs and altered N availability. Loss of *Sphagnum* at S1 Bog with warming has likely reduced N fixation inputs and altered surface soil N and P cycling since *Sphagnum* biomass represents a large, nutrient-rich pool that will decompose quickly under warm and dry conditions. Accelerated turnover of acrotelm N and P may result in losses of N and P to denitrification and lateral outflow, but we expect that enhanced uptake by shrubs and trees will partially offset these fluxes. N fixation inputs were low compared to rates of N deposition and the size of the *Sphagnum* biomass N so we do not expect reduction of N fixation to decrease N availability in the immediate future.

Conclusions

Analysis of N and P cycling within an ombrotrophic bog in northern Minnesota highlights the importance of belowground ecosystem components. Organic soils stored over 98% of N and P at this site, and fine roots in the upper aerobic acrotelm contained pools of N and P that were similar in size to leaf N and P pools. Plants generally had twice as much biomass aboveground than below, but the proportion of belowground biomass was higher for understory species. Trees, in addition to having a greater proportion of their biomass N and P aboveground, cycled nutrients more slowly than understory plants and *Sphagnum*. Whole-plant N:P ratios demonstrated differential limitation of N versus P across PFTs, with trees exhibiting the highest degree of N limitation. On an annual basis, N was accumulating in the ecosystem at $0.2 \pm 0.1 \text{ g N m}^{-2} \text{ year}^{-1}$ and net fluxes of P were near zero. Annual cycling of N and P through vegetation shows that *Sphagnum* represents a large and dynamic pool of N and P at the S1 Bog that is vulnerable to the impacts

of both manipulative and regional warming. ELM-SPRUCE accurately captured N but not P cycling across PFTs, and mismatches between modelled and measured pools of *Sphagnum* biomass N and P were explained by the differing definitions of live *Sphagnum* tissue. Analysis of N versus P cycling within an ombrotrophic bog using both empirical data collection and an ESM represents a step toward understanding the complex behavior of nutrient-limited peatland ecosystems.

Supplementary Information The online version contains supplementary material available at <https://doi.org/10.1007/s11104-021-05065-x>.

Acknowledgements We would like to thank Robert Nettles, Kyle Pearson, Ryan Heiderman, Leslie A. Hook, Holly Vander Stel, Anna Jensen, Eric Ward, Keith Oleheiser, Anne Gapinski, Mitchell Olds, Madeline Wiley, Leigh Kastenson, Reid Peterson, Ben Munson, Anna Hall, Dustin Woodruff and Stan D. Wullschleger for helping with field data collection and lab work. The authors from ORNL are supported by the U.S. Department of Energy, Office of Science, Office of Biological and Environmental Research. ORNL is managed by UT-Battelle, LLC, for the DOE under contract DE-AC05-1008 00OR22725. The USDA Forest Service funded contributions of SDS and RKK in support of the SPRUCE Experiment. This work was supported in part by a grant from the National Science Foundation (DEB 1754756) to JEK. Nathan Armistead (ORNL) helped conceptualize and construct Figure 1. This manuscript was significantly improved by comments from two anonymous reviewers and Tim Moore (McGill University).

This manuscript has been authored by UT-Battelle, LLC, under contract DE-AC05-00OR22725 with the US Department of Energy (DOE). The US government retains and the publisher, by accepting the article for publication, acknowledges that the US government retains a nonexclusive, paid-up, irrevocable, worldwide license to publish or reproduce the published form of this manuscript, or allow others to do so, for US government purposes. DOE will provide public access to these results of federally sponsored research in accordance with the DOE Public Access Plan (<http://energy.gov/downloads/doe-public-access-plan>).

Author contribution VGS collated and analyzed data, wrote the manuscript and incorporated feedback from SB, NAG, KH, CMI, TMJ, RK, JK, AM, RJN, JRP, DR, CWS, SS, XS, AW, JW, DW, XY, and PRH. JG, DR, XS, and XY contributed novel methods and/or model simulations. SB, JG, NAG, TMJ, JK, AM, and SS analyzed data. All authors performed research, conceived of this study, and/or provided substantive feedback on the manuscript and analysis.

Data availability Data associated with this manuscript are publicly available and full citations for data products are listed under “References to data products and documentation” Throughout the text, citations for data products will be

annotated with “*data citation*” to differentiate them from literature citations. Table 1 also includes DOIs and hyperlinks to specific data products included in this analysis.

Declarations

Conflict of interests The authors have no conflict of interest.

References to data products and documentation

- emmeans*: estimated Marginal Means, aka Least-Squares Means. Russell Lenth (2020) R package version 1.4.6. <https://CRAN.R-project.org/package=emmeans>
- Graham JD, Glenn NF, Spaete LP (2019) SPRUCE terrestrial laser scanning of experimental plots beginning in 2015. Oak Ridge National Laboratory, TES SFA, U.S. Department of Energy, Oak Ridge, Tennessee, U.S.A. <https://doi.org/10.25581/spruce.067/1515552>
- Hanson PJ, Riggs JS, Dorrance C, Nettles WR, Hook LA (2015) SPRUCE environmental monitoring data: 2010–2016. Carbon Dioxide Information Analysis Center, Oak Ridge National Laboratory, U.S. Department of Energy, Oak Ridge, Tennessee, U.S.A. <https://doi.org/10.3334/CDIAC/spruce.001>
- Hanson PJ, Phillips JR, Wullschlegel SD, Nettles WR, Warren JM, Ward EJ, Graham JD (2018a) SPRUCE tree growth assessments of picea and larch in S1-bog plots and SPRUCE experimental plots beginning in 2011. Oak Ridge National Laboratory, TES SFA, U.S. Department of Energy, Oak Ridge, Tennessee, U.S.A. <https://doi.org/10.25581/spruce.051/1433836>
- Hanson PJ, Phillips JR, Brice DJ, Hook LA (2018b) SPRUCE Shrub-Layer Growth Assessments in S1-Bog Plots and SPRUCE Experimental Plots beginning in 2010. Oak Ridge National Laboratory, TES SFA, U.S. Department of Energy, Oak Ridge, Tennessee, U.S.A. <https://doi.org/10.25581/spruce.052/1433837>
- Heiderman RR, Nettles WR, Ontl TA, Latimer JM, Richardson AD, Hanson PJ (2018) SPRUCE manual phenology observations and photographs beginning in 2010. Oak Ridge National Laboratory, TES SFA, U.S. Department of Energy, Oak Ridge, Tennessee, U.S.A. <https://doi.org/10.25581/spruce.054/1444106>
- Iversen CM, Hanson PJ, Brice DJ, Phillips JR, McFarlane KJ, Hobbie EA, Kolka RK (2014) SPRUCE peat physical and chemical characteristics from experimental plot cores, 2012. Oak Ridge National Laboratory, TES SFA, U.S.A. <https://doi.org/10.3334/CDIAC/spruce.005>
- Iversen CM, Powell AS, McCormack ML, Blackwood CB, Fretschel GT, Kattge J, Roumet C, Stover DB, Soudzilovskaia NA, Valverde-Barrantes OJ, van Bodegom PM, Violle C (2018) Fine-root ecology database (FRED): a global collection of root trait data with coincident site, vegetation, edaphic, and climatic data, version 2. Oak Ridge National Laboratory, TES SFA, U.S. Department of Energy, Oak Ridge, Tennessee, U.S.A. <https://doi.org/10.25581/ornlsfa.012/1417481>
- Iversen CM, Brice DJ, Childs J, Vander Stel HM, Salmon VG (2021) SPRUCE S1 bog production of newly-grown fine roots assessed using root ingrowth cores in 2013. Oak Ridge National Laboratory, TES SFA, U.S. Department of Energy, Oak Ridge, Tennessee, U.S.A. <https://doi.org/10.25581/spruce.091/1782483>
- Jensen AM, Warren JM, Hook LA, Wullschlegel SD, Brice DJ, Childs J, Vander Stel HM (2018) SPRUCE S1 bog pretreatment seasonal photosynthesis and respiration of trees, shrubs, and herbaceous plants, 2010–2015. Oak Ridge National Laboratory, TES SFA, U.S. Department of Energy, Oak Ridge, Tennessee, U.S.A. <https://doi.org/10.3334/CDIAC/spruce.008>
- Malhotra A, Brice DJ, Childs J, Vander Stel HM, Bellaire SE, Kraeske E, Letourneau SM, Owens L, Rasnake LM, Iversen CM (2020) SPRUCE production and chemistry of newly-grown fine roots assessed using root ingrowth cores in SPRUCE experimental plots beginning in 2014. Oak Ridge National Laboratory, TES SFA, U.S. Department of Energy, Oak Ridge, Tennessee, U.S.A. <https://doi.org/10.25581/spruce.077/1607860>
- Norby RJ, Childs J (2018) SPRUCE: sphagnum productivity and community composition in the SPRUCE experimental plots. Oak Ridge National Laboratory, TES SFA, U.S. Department of Energy, Oak Ridge, Tennessee, U.S.A. <https://doi.org/10.25581/spruce.049/1426474>
- Norby RJ, Childs J, Brice D (2020) SPRUCE: sphagnum carbon, nitrogen and phosphorus concentrations in the SPRUCE experimental plots. Oak Ridge National Laboratory, TES SFA, U.S. Department of Energy, Oak Ridge, Tennessee, U.S.A. <https://doi.org/10.25581/spruce.084/1647361>
- Phillips JR, Brice DJ, Hanson PJ, Childs J, Iversen CM, Norby RJ, Warren JM (2017) SPRUCE pretreatment plant tissue analyses, 2009 through 2013. Oak Ridge National Laboratory, TES SFA, U.S. Department of Energy, Oak Ridge, Tennessee, U.S.A. <https://doi.org/10.3334/CDIAC/spruce.038>
- Phillips JR, Hanson PJ, Warren JM (2021) SPRUCE plant tissue analyses from experimental plots beginning 2017. Oak Ridge National Laboratory, TES SFA, U.S. Department of Energy, Oak Ridge, Tennessee, U.S.A. <https://doi.org/10.25581/spruce.090/1780604>
- R Core Team (2020) R: a language and environment for statistical computing. <https://www.r-project.org/>
- Sebestyen SD, Griffiths NA (2016) SPRUCE enclosure corral and sump system: description, operation, and calibration. Climate Change Science Institute, Oak Ridge National Laboratory, U.S. Department of Energy, Oak Ridge, Tennessee, U.S.A. <https://doi.org/10.3334/CDIAC/spruce.030>
- Sebestyen SD, Funke MM, Cotner J, Larson JT, Aspelin NA (2017) Water chemistry data for studies of the biodegradability of dissolved organic matter in peatland catchments at the Marcell Experimental Forest: 2009–2011, Forest Service Research Data Archive, Fort Collins, CO. <https://doi.org/10.2737/RDS-2017-0067>
- Sebestyen SD, Griffiths NA, Oleheiser KC, Stelling JM (2020) SPRUCE precipitation chemistry and bulk atmospheric deposition beginning in 2013. Oak Ridge National Laboratory, TES SFA, U.S. Department of Energy, Oak Ridge,

Tennessee, U.S.A. <https://doi.org/10.25581/spruce.085/1664397>

- Sebestyen SD, Griffiths NA, Oleheiser KC, Stelling JM, Pierce CE, Nater EA, Wilson RM, Chanton JP, Hall SJ, Curtinrich HJ, Toner BM, Kolka RK (2021) SPRUCE outflow chemistry data for experimental plots beginning in 2016. Oak Ridge National Laboratory, TES SFA, U.S. Department of Energy, Oak Ridge, Tennessee, U.S.A. <https://doi.org/10.25581/spruce.088/1775142>
- Verry ES (2018) Marcell experimental watersheds 1968 vegetation survey data. Fort Collins, CO: Forest Service Research Data Archive. <https://doi.org/10.2737/RDS-2018-0016>

References to peer-reviewed literature

- Achat DL, Augusto L, Gallet-Budynek A, Loustau D (2016) Future challenges in coupled C-N-P cycle models for terrestrial ecosystems under global change: a review. *Biogeochemistry* 131:173–202. <https://doi.org/10.1007/s10533-016-0274-9>
- Aerts R, Verhoeven JTA, Whigham DF (1999) Plant-mediated controls on nutrient cycling in temperate fens and bogs. *Ecology* 80:2170–2181. [https://doi.org/10.1890/0012-9658\(1999\)080\[2170:PMCONC\]2.0.CO;2](https://doi.org/10.1890/0012-9658(1999)080[2170:PMCONC]2.0.CO;2)
- Aerts R, Wallen B, Malmer N (1992) Growth-limiting nutrients in *Sphagnum*-dominated bogs subject to low and high atmospheric nitrogen supply. *J Ecol* 80:131. <https://doi.org/10.2307/2261070>
- Aldous AR (2002a) Nitrogen retention by *Sphagnum mosses*: responses to atmospheric nitrogen deposition and drought. *Can J Bot* 80:721–731. <https://doi.org/10.1139/b02-054>
- Aldous AR (2002b) Nitrogen translocation in *Sphagnum mosses*: effects of atmospheric nitrogen deposition. *New Phytol* 156:241–253. <https://doi.org/10.1046/j.1469-8137.2002.00518.x>
- Alm J, Schulman L, Walden J et al (1999) Carbon balance of a boreal bog during a year with an exceptionally dry summer. *Ecology* 80:161–174. [https://doi.org/10.1890/0012-9658\(1999\)080\[0161:CBOABB\]2.0.CO;2](https://doi.org/10.1890/0012-9658(1999)080[0161:CBOABB]2.0.CO;2)
- Bares RH, Wali MK (1979) Chemical relations and litter production of *Picea mariana* and *Larix laricina* stands on an alkaline peatland in Northern Minnesota. *Vegetatio* 40:79–94. <https://doi.org/10.1007/BF00055837>
- Bond-Lamberty B, Wang C, Gower ST (2002) Aboveground and belowground biomass and sapwood area allometric equations for six boreal tree species of northern Manitoba. *Can J for Res* 32:1441–1450. <https://doi.org/10.1139/x02-063>
- Bragazza L, Parisod J, Buttler A, Bardgett RD (2013) Biogeochemical plant-soil microbe feedback in response to climate warming in peatlands. *Nat Clim Chang* 3:273–277. <https://doi.org/10.1038/nclimate1781>
- Bragazza L, Bardgett RD, Mitchell EAD, Buttler A (2015) Linking soil microbial communities to vascular plant abundance along a climate gradient. *New Phytol* 205:1175–1182. <https://doi.org/10.1111/nph.13116>
- Bragazza L, Buttler A, Robroek BJM et al (2016) Persistent high temperature and low precipitation reduce peat carbon accumulation. *Glob Change Biol* 22:4114–4123. <https://doi.org/10.1111/gcb.13319>
- Bridgham SD, Pastor J, Janssens JA et al (1996) Multiple limiting gradients in peatlands: a call for a new paradigm. *Wetlands* 16:45–65. <https://doi.org/10.1007/BF03160645>
- Bridgham SD, Updegraff K, Pastor J (1998) Carbon, nitrogen, and phosphorus mineralization in northern wetlands. *Ecology* 79:1545–1561. [https://doi.org/10.1890/0012-9658\(1998\)079\[1545:CNAPMI\]2.0.CO;2](https://doi.org/10.1890/0012-9658(1998)079[1545:CNAPMI]2.0.CO;2)
- Carrell AA, Kolton M, Glass JB et al (2019) Experimental warming alters the community composition, diversity, and N₂ fixation activity of peat moss (*Sphagnum fallax*) microbiomes. *Glob Change Biol*. <https://doi.org/10.1111/gcb.14715>
- Chapin CT, Bridgham SD, Pastor J, Updegraff K (2003) Nitrogen, phosphorus, and carbon mineralization in response to nutrient and lime additions in peatlands. *Soil Sci* 168:409–420. <https://doi.org/10.1097/01.ss.0000075286.87447.5d>
- Cleveland CC, Liptzin D (2007) C:N: P stoichiometry in soil: is there a “Redfield ratio” for the microbial biomass? *Biogeochemistry* 85:235–252. <https://doi.org/10.1007/s10533-007-9132-0>
- Dorrepaal E, Toet S, van Logtestijn RSP et al (2009) Carbon respiration from subsurface peat accelerated by climate warming in the subarctic. *Nature* 460:616–619. <https://doi.org/10.1038/nature08216>
- Elser JJ, Fagan WF, Kerkhoff AJ et al (2010) Biological stoichiometry of plant production: metabolism, scaling and ecological response to global change. *New Phytol* 186:593–608. <https://doi.org/10.1111/j.1469-8137.2010.03214.x>
- Frolking S, Roulet NT (2007) Holocene radiative forcing impact of northern peatland carbon accumulation and methane emissions. *Glob Change Biol* 13:1079–1088. <https://doi.org/10.1111/j.1365-2486.2007.01339.x>
- Griffiths NA, Sebestyen SD (2016) Dynamic vertical profiles of peat porewater chemistry in a northern peatland. *Wetlands* 36:1119–1130. <https://doi.org/10.1007/s13157-016-0829-5>
- Griffiths NA, Hanson PJ, Ricciuto DM et al (2017) Temporal and spatial variation in peatland carbon cycling and implications for interpreting responses of an ecosystem-scale warming experiment. *Soil Sci Soc Am J* 81:1668–1688. <https://doi.org/10.2136/sssaj2016.12.0422>
- Groffman PM, Altabet MA, Böhlke JK et al (2006) Methods for measuring denitrification: diverse approaches to a difficult problem. *Ecol Appl* 16:2091–2122. [https://doi.org/10.1890/1051-0761\(2006\)016\[2091:MFMDDA\]2.0.CO;2](https://doi.org/10.1890/1051-0761(2006)016[2091:MFMDDA]2.0.CO;2)
- Güsewell S (2004) N: P ratios in terrestrial plants: variation and functional significance. *New Phytol* 164:243–266. <https://doi.org/10.1111/j.1469-8137.2004.01192.x>
- Güsewell S, Koerselman W (2002) Variation in nitrogen and phosphorus concentrations of wetland plants. *Perspect Plant Ecol Evol Syst* 5:37–61. <https://doi.org/10.1078/1433-8319-0000022>
- Hanson PJ, Riggs JS, Robert Nettles W et al (2017) Attaining whole-ecosystem warming using air and deep-soil heating methods with an elevated CO₂ atmosphere. *Biogeosciences* 14:861–883. <https://doi.org/10.5194/bg-14-861-2017>

- Hanson PJ, Griffiths NA, Iversen CM et al (2020) Rapid net carbon loss from a whole-ecosystem warmed peatland. *AGU Adv*. <https://doi.org/10.1029/2020av000163>
- Hill BH, Elonen CM, Jicha TM et al (2014) Ecoenzymatic stoichiometry and microbial processing of organic matter in northern bogs and fens reveals a common P-limitation between peatland types. *Biogeochemistry* 120:203–224. <https://doi.org/10.1007/s10533-014-9991-0>
- Hill BH, Jicha TM, Lehto LRLP et al (2016) Comparisons of soil nitrogen mass balances for an ombrotrophic bog and a minerotrophic fen in northern Minnesota. *Sci Total Environ* 550:880–892. <https://doi.org/10.1016/j.scitotenv.2016.01.178>
- Hopple AM, Wilson RM, Kolton M et al (2020) Massive peatland carbon banks vulnerable to rising temperatures. *Nat Commun* 11:4–10. <https://doi.org/10.1038/s41467-020-16311-8>
- Iversen CM, Bridgham SD, Kellogg LE (2010) Scaling plant nitrogen use and uptake efficiencies in response to nutrient addition in peatlands. *Ecology* 91:693–707. <https://doi.org/10.1890/09-0064.1>
- Iversen CM, Childs J, Norby RJ et al (2018b) Fine-root growth in a forested bog is seasonally dynamic, but shallowly distributed in nutrient-poor peat. *Plant Soil*. <https://doi.org/10.1007/s11104-017-3231-z>
- Jensen AM, Warren JM, Hanson PJ et al (2015) Needle age and season influence photosynthetic temperature response and total annual carbon uptake in mature *Picea mariana* trees. *Ann Bot* 116:821–832. <https://doi.org/10.1093/aob/mcv115>
- Jensen AM, Warren JM, King AW et al (2019) Simulated projections of boreal forest peatland ecosystem productivity are sensitive to observed seasonality in leaf physiology. *Tree Physiol* 39:556–572. <https://doi.org/10.1093/treephys/tpy140>
- Johnson MG, Tingey DT, Phillips DL, Storm MJ (2001) Advancing fine root research with minirhizotrons. *Environ Exp Bot* 45:263–289. [https://doi.org/10.1016/S0098-8472\(01\)00077-6](https://doi.org/10.1016/S0098-8472(01)00077-6)
- Juutinen S, Bubier JL, Moore TR (2010) Responses of vegetation and ecosystem CO₂ exchange to 9 years of nutrient addition at mer bleue bog. *Ecosystems* 13:874–887. <https://doi.org/10.1007/s10021-010-9361-2>
- Klimešová J, Martínková J, Ottaviani G (2018) Belowground plant functional ecology: towards an integrated perspective. *Funct Ecol*. <https://doi.org/10.1111/1365-2435.13145>
- Kluber L, Johnston E, Allen S et al (2020) Constraints on microbial communities, decomposition and methane production in deep peat deposits. *PLoS ONE*. <https://doi.org/10.1371/journal.pone.0223744>
- Koerselman W, Meuleman AFM (1996) The vegetation N: P ratio: a new tool to detect the nature of nutrient limitation. *J Appl Ecol* 33:1441–1450
- Kolka R, Sebestyen S, Verry ES, Brooks K (2011) Peatland biogeochemistry and watershed hydrology at the marcell experimental forest. CRC Press
- Krab EJ, Cornelissen JHC, Lang SI, Van Logtestijn RSP (2008) Amino acid uptake among wide-ranging moss species may contribute to their strong position in higher-latitude ecosystems. *Plant Soil* 304:199–208. <https://doi.org/10.1007/s11104-008-9540-5>
- Lamhamedi MS, Bernier PYP (1994) Ecophysiology and field performance of black spruce (*Picea mariana*): a review. *Ann Sci for* 51:529–551. <https://doi.org/10.1051/forest:19940601>
- Lin X, Tfaily MM, Green SJ et al (2014) Microbial metabolic potential for carbon degradation and nutrient (nitrogen and phosphorus) acquisition in an ombrotrophic peatland. *Appl Environ Microbiol* 80:3531–3540. <https://doi.org/10.1128/AEM.00206-14>
- Malhotra A, Brice DJ, Childs J et al (2020b) Peatland warming strongly increases fine-root growth. *Proc Natl Acad Sci* 117:17627–17634. <https://doi.org/10.1073/pnas.2003361117>
- McKane RB, Johnson LC, Shaver GR et al (2002) Resource-based niche provide a basis for plant species diversity and dominance in arctic tundra. *Nature* 415:68–71
- McPartland MY, Montgomery RA, Hanson PJ et al (2020) Vascular plant species response to warming and elevated carbon dioxide in a boreal peatland. *Environ Res Lett*. <https://doi.org/10.1088/1748-9326/abc4fb>
- Moore TR (1989) Growth and net production of Sphagnum at five fen sites, subarctic eastern Canada. *Can J Bot* 67:1203–1207. <https://doi.org/10.1139/b89-156>
- Moore T, Blodau C, Turunen J et al (2004) Patterns of nitrogen and sulfur accumulation and retention in ombrotrophic bogs, eastern Canada. *Glob Change Biol* 11:356–367. <https://doi.org/10.1111/j.1365-2486.2004.00882.x>
- Moore TR, Alfonso A, Clarkson BR (2018) Plant uptake of organic nitrogen in two peatlands. *Plant Soil* 433:391–400. <https://doi.org/10.1007/s11104-018-3851-y>
- Nichols JE, Peteet DM (2019) Rapid expansion of northern peatlands and doubled estimate of carbon storage. *Nat Geosci* 12:917–921. <https://doi.org/10.1038/s41561-019-0454-z>
- Norby RJ, Childs J, Hanson PJ, Warren JM (2019) Rapid loss of an ecosystem engineer: *Sphagnum* decline in an experimentally warmed bog. *Ecol Evol* 9:12571–12585. <https://doi.org/10.1002/ece3.5722>
- Read DJ, Leake JR, Perez-Moreno J (2004) Mycorrhizal fungi as drivers of ecosystem processes in heathland and boreal forest biomes. *Can J Bot*. <https://doi.org/10.1139/b04-123>
- Reiners WA (1986) Complementary models for ecosystems. *Am Nat* 127:59–73. <https://doi.org/10.1086/284467>
- Rustad LE, Campbell JL, Marion GM et al (2001) A meta-analysis of the response of soil respiration, net nitrogen mineralization, and aboveground plant growth to experimental ecosystem warming. *Oecologia* 126:543–562. <https://doi.org/10.1007/s004420000544>
- Scharlemann JPW, Tanner EVJ, Hiederer R, Kapos V (2014) Global soil carbon: understanding and managing the largest terrestrial carbon pool. *Carbon Manag* 5:81–91. <https://doi.org/10.4155/cmt.13.77>
- Schimel JP, Bennet J, Bennett JB (2004) Nitrogen mineralization: challenges of a changing paradigm. *Ecology* 85:591–602. <https://doi.org/10.1890/03-8024>
- Searle SR, Speed FM, Milliken GA (1980) Population marginal means in the linear model: an alternative to least squares means. *Am Stat* 34:216–221
- Sebestyen SD, Dorrance C, Olson DM et al (2011) Long-term monitoring sites and trends at the Marcell Experimental Forest. *Peatland biogeochemistry and watershed*

- hydrology at the Marcell Experimental Forest. CRC Press, Boca Raton, pp 15–71
- Sebestyen SD, Lany NK, Roman DT et al (2021b) Hydrological and meteorological data from research catchments at the Marcell Experimental Forest, Minnesota, USA. *Hydrol Process* 35:e14092. <https://doi.org/10.1002/hyp.14092>
- Sgouridis F, Stott A, Ullah S (2016) Application of the 15N gas-flux method for measuring in situ N₂ and N₂O fluxes due to denitrification in natural and semi-natural terrestrial ecosystems and comparison with the acetylene inhibition technique. *Biogeosciences* 13:1821–1835. <https://doi.org/10.5194/bg-13-1821-2016>
- Shi X, Thornton PE, Ricciuto DM et al (2015) Representing northern peatland microtopography and hydrology within the Community Land Model. *Biogeosciences* 12:6463–6477. <https://doi.org/10.5194/bg-12-6463-2015>
- Shi X, Ricciuto DM, Thornton PE et al (2021) Extending a land-surface model with *Sphagnum* moss to simulate responses of a northern temperate bog to whole ecosystem warming and elevated CO₂. *Biogeosciences* 18:467–486. <https://doi.org/10.5194/bg-18-467-2021>
- Steinweg JM, Kostka JE, Hanson PJ, Schadt CW (2018) Temperature sensitivity of extracellular enzymes differs with peat depth but not with season in an ombrotrophic bog. *Soil Biol Biochem* 125:244–250. <https://doi.org/10.1016/j.soilbio.2018.07.001>
- Sterner RW, Elser JJ (2002) *Ecological Stoichiometry: the biology of elements from molecules to the biosphere*. Princeton University Press, Princeton
- Tfaily MM, Cooper WT, Kostka JE et al (2014) Organic matter transformation in the peat column at Marcell Experimental Forest: Humification and vertical stratification. *J Geophys Res Biogeosci* 119:661–675. <https://doi.org/10.1002/2013JG002492>
- Thomas RQ, Brookshire ENJ, Gerber S (2015) Nitrogen limitation on land: how can it occur in Earth system models? *Glob Change Biol* 21:1777–1793. <https://doi.org/10.1111/gcb.12813>
- Urban NR, Eisenreich SJ (1988) Nitrogen cycling in a forested Minnesota bog. *Can J Bot* 66:435–449. <https://doi.org/10.1139/b88-069>
- Urban NR, Eisenreich SJ, Bayley SE (1988) The relative importance of denitrification and nitrate assimilation in midcontinental bogs. *Limnol Oceanogr* 33:1611–1617. <https://doi.org/10.4319/lo.1988.33.6part2.1611>
- Verry ES, Boelter DH, Päivänen J et al (2011) *Physical properties of organic soils. Peatland biogeochemistry and watershed hydrology at the Marcell Experimental Forest*. CRC Press, New York, pp 135–176
- Vile MA, Kelman Wieder R, Živković T et al (2014) N₂-fixation by methanotrophs sustains carbon and nitrogen accumulation in pristine peatlands. *Biogeochemistry* 121:317–328. <https://doi.org/10.1007/s10533-014-0019-6>
- Vitousek PM (1982) Nutrient cycling and nutrient use efficiency. *Am Nat* 119:553–572
- Wang M, Moore TR, Talbot J, Richard PJH (2014a) The cascade of C:N: P stoichiometry in an ombrotrophic peatland: From plants to peat. *Environ Res Lett*. <https://doi.org/10.1088/1748-9326/9/2/024003>
- Wang M, Murphy MT, Moore TR (2014b) Nutrient resorption of two evergreen shrubs in response to long-term fertilization in a bog. *Oecologia* 174:365–377. <https://doi.org/10.1007/s00442-013-2784-7>
- Warren MJ, Lin X, Gaby JC et al (2017) Molybdenum-based diazotrophy in a *Sphagnum* peatland in northern Minnesota. *Appl Environ Microbiol* 83:1–14. <https://doi.org/10.1128/AEM.01174-17>
- Wieder RK, Scott KD, Kamminga K et al (2009) Postfire carbon balance in boreal bogs of Alberta, Canada. *Glob Change Biol* 15:63–81. <https://doi.org/10.1111/j.1365-2486.2008.01756.x>
- Wu J, Roulet NT, Sagerfors J, Nilsson MB (2013) Simulation of six years of carbon fluxes for a sedge-dominated oligotrophic minerogenic peatland in Northern Sweden using the McGill Wetland Model (MWM). *J Geophys Res Biogeosci* 118:795–807. <https://doi.org/10.1002/jgrg.20045>
- Yu ZC (2012) Northern peatland carbon stocks and dynamics: a review. *Biogeosciences* 9:4071–4085. <https://doi.org/10.5194/bg-9-4071-2012>
- Živković T, Disney K, Moore TR (2017) Variations in nitrogen, phosphorus, and δ¹⁵n in sphagnum mosses along a climatic and atmospheric deposition gradient in eastern Canada. *Botany* 95:829–839. <https://doi.org/10.1139/cjb-2016-0314>

Publisher's Note Springer Nature remains neutral with regard to jurisdictional claims in published maps and institutional affiliations.